

ZEROTH-ORDER OPTIMIZATION MEETS HUMAN FEEDBACK: PROVABLE LEARNING VIA RANKING ORACLES

Zhiwei Tang

zhiweitang1@link.cuhk.edu.cn

Dmitry Rybin

dmitryrybin@link.cuhk.edu.cn

Tsung-Hui Chang

changtsunghui@cuhk.edu.cn

The Chinese University of Hong Kong, Shenzhen

March 8, 2023

ABSTRACT

In this paper, we focus on a novel optimization problem in which the objective function is a black-box and can only be evaluated through a ranking oracle. This problem is common in real-world applications, particularly in cases where the function is assessed by human judges. Reinforcement Learning with Human Feedback (RLHF) is a prominent example of such an application, which is adopted by the recent works [24, 18, 23, 1] to improve the quality of Large Language Models (LLMs) with human guidance. We propose ZO-RankSGD, a first-of-its-kind zeroth-order optimization algorithm, to solve this optimization problem with a theoretical guarantee. Specifically, our algorithm employs a new rank-based random estimator for the descent direction and is proven to converge to a stationary point. ZO-RankSGD can also be directly applied to the policy search problem in reinforcement learning when only a ranking oracle of the episode reward is available. This makes ZO-RankSGD a promising alternative to existing RLHF methods, as it optimizes in an online fashion and thus can work without any pre-collected data. Furthermore, we demonstrate the effectiveness of ZO-RankSGD in a novel application: improving the quality of images generated by a diffusion generative model with human ranking feedback. Throughout experiments, we found that ZO-RankSGD can significantly enhance the detail of generated images with only a few rounds of human feedback. Overall, our work advances the field of zeroth-order optimization by addressing the problem of optimizing functions with only ranking feedback, and offers an effective approach for aligning human and machine intentions in a wide range of domains. Our code is released here <https://github.com/TZW1998/Taming-Stable-Diffusion-with-Human-Ranking-Feedback>.

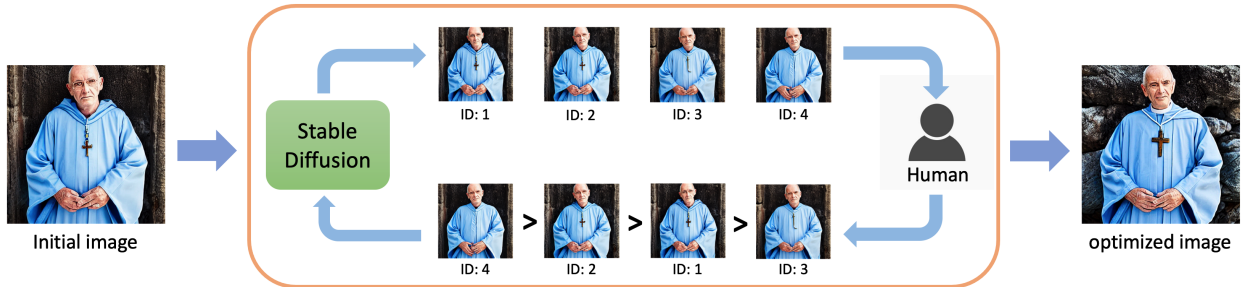


Figure 1: Application of our proposed algorithm on enhancing the quality of images generated from Stable diffusion [29] with human ranking feedback. At each iteration of this human-in-the-loop optimization, we use Stable Diffusion to generate multiple images by perturbing the latent embedding with random noise, which are then ranked by humans based on their quality. After that, the ranking information is leveraged to update the latent embedding.

1 Introduction

Ranking data is an omnipresent feature of the internet, appearing on a variety of platforms and applications, such as search engines, social media feeds, online marketplaces, and review sites. It plays a crucial role in how we navigate and make sense of the vast amount of information available online. Moreover, ranking information has a unique appeal to humans, as it enables them to express their personal preferences in a straightforward and intuitive way [24, 18, 23, 1]. The significance of ranking data becomes even more apparent when some objective functions are evaluated through human beings, which is becoming increasingly common in various applications. Assigning an exact score or rating can often require a significant amount of cognitive burden or domain knowledge, making it impractical for human evaluators to provide precise feedback. In contrast, a ranking-based approach can be more natural and straightforward, allowing human evaluators to express their preferences and judgments with ease.

In this context, our paper studies an important optimization problem where the objective function can only be accessed via a ranking oracle.

1.1 Problem formulation

With an objective function $f : \mathbb{R}^d \rightarrow \mathbb{R}$, we focus on the following optimization problem:

$$\min_{x \in \mathbb{R}^d} f(x), \quad (1)$$

where f is a black-box function, and we can only query it via a ranking oracle that can sort every input based on the values of f . In this work, we focus on a particular family of ranking oracles where only the sorted indexes of top elements are returned. Such oracles are acknowledged to be natural for human decision-making [15]. We formally define this kind of oracle as follows:

Definition 1 ((m, k) -ranking oracle). *Given a function $f : \mathbb{R}^d \rightarrow \mathbb{R}$ and m points x_1, \dots, x_m to query, an (m, k) ranking oracle $O_f^{(m,k)}$ will return k smallest points sorted in their order. For example, if $O_f^{(m,k)}(x_1, \dots, x_m) = (i_1, \dots, i_k)$, then*

$$f(x_{i_1}) \leq f(x_{i_2}) \leq \dots \leq f(x_{i_k}) \leq \min_{j \notin \{i_1, \dots, i_k\}} f(x_j).$$

1.2 Applications

The optimization problem (1) with a (m, k) -ranking oracle is a common feature in many real-world applications, especially when the objective function f is evaluated by human judges. One prominent example of this type of problem is found in the growing field of Reinforcement Learning with Human Feedback (RLHF) [24, 18, 23, 1], where human evaluators are asked to rank generated text according to their personal preferences, with an aim to improve the generation quality of Large Language Models (LLMs). Inspired by these works, in Section 4, we propose a similar application in which human feedback is used to enhance the quality of images generated by Stable Diffusion [29], a state-of-the-art text-to-image generative model. An overview of this application is demonstrated in Figure 1.

Beyond human feedback, ranking oracles have the potential to be useful in many other applications. For instance, in cases where the information in the values of f must remain private, ranking data may provide a more secure and confidential option for data sharing and analysis. This is particularly relevant in sensitive domains, such as healthcare or finance, where the exact value of personal information must be protected.

Moreover, obtaining rank data may be cheaper and easier than obtaining exact function values in many cases, such as when optimizing the hyperparameters of a machine learning model [19, 17]. In these situations, obtaining rank data requires less time and resources than obtaining precise performance measures on validation datasets, making it an attractive option for optimizing complex models with limited computational budgets.

1.3 Related works

Zerоth-Order Optimization. Zerоth-order optimization, also known as derivative-free or black-box optimization, has been a topic of extensive study in the optimization literature for several decades, with notable examples including the Nelder-Mead Simplex method [21], Bayesian optimization [10], Direct Search [11] and random approximation methods [22]. However, most existing works in this area assume that the objective function value is directly accessible, and the optimization is performed based on this value, which is not appropriate for our setting where only ranking information is available. Several heuristic algorithms have been proposed that rely solely on ranking information, such as CMA-ES [19], but these methods lack theoretical guarantees and may perform poorly in practice.

The most closely related work to ours is the recent study by [3], which investigates zeroth-order optimization via a comparison oracle that returns the sign of the difference in function values between two points. In fact, this comparison oracle is equivalent to $(2, 1)$ -ranking oracle, which is a special case of the (m, k) -ranking oracle considered in our work. Generally speaking, the approach in [3] aims to recover the gradient of the objective function using 1-bit compressive sensing techniques [25]. However, this approach is limited to convex objective functions and is not applicable to non-convex functions.

In contrast to [3], our work considers a more general (m, k) -ranking oracle and extends the scope to non-convex functions. Besides, our approach does not rely on any compressive sensing techniques and instead provides a novel theoretical analysis that can characterize the expected convergence behavior of our proposed algorithm.

Relationship to RLHF. Reinforcement Learning with Human Feedback (RLHF) is a relatively new and rapidly growing field that has shown significant promise in aligning the intentions of humans and machines [24, 18, 23, 1]. The general approach in RLHF involves collecting ranking data from humans to train a reward model, which is then used to fine-tune a pre-trained model with policy gradients. However, this method faces two main challenges. First, it requires a large amount of ranking data to be collected before fine-tuning can begin, which can be time-consuming and expensive, particularly for smaller organizations. Second, the interaction with humans, or the ranking oracle, occurs only once and does not allow for the ongoing ranking of the model’s output, limiting the potential for continued model improvement.

Our proposed zeroth-order optimization algorithm, which can be directly applied to policy search in reinforcement learning, can be a promising alternative to existing RLHF methods as it allows for the collection of ranking data in an online fashion. This overcomes the challenges of the traditional RLHF approach by enabling the model’s performance to be continuously improved without any pre-collected data. On the other hand, our algorithm can also serve as a process for data collection while optimizing the objective function, which can better facilitate small organizations to build models from scratch.

1.4 Contributions in this work

Our main contributions are summarized as follows:

- (1) **The first rank-based zeroth-order optimization algorithm with a theoretical guarantee.** We present an innovative method for optimizing objective functions via their ranking oracles. Our proposed algorithm is based on a new rank-based stochastic estimator for descent direction and is proven to converge to a stationary point. Additionally, we provide a rigorous analysis of how various ranking oracles can impact the convergence rate by employing a novel variance analysis.
- (2) **A promising alternative to RLHF.** We also show that our algorithm is applicable to policy search in reinforcement learning when only a ranking oracle of the environment reward is available. In comparison to existing RLHF approaches, Our algorithm facilitates the real-time acquisition of ranking data, which leads to continuous improvement of the model’s performance without requiring any pre-collected data.
- (3) **A way to tame diffusion generative models with human feedback.** We also apply our algorithm to a novel application: improving the quality of images generated by Stable Diffusion [29] with human ranking feedback. Our algorithm is shown to significantly enhance the details of the generated images, providing a new perspective on how to use human feedback to improve the performance of diffusion models.

Overall, our work advances the field of zeroth-order optimization by addressing the problem of optimizing functions where only ranking feedback of them is available. Furthermore, our algorithm offers a new and effective approach for aligning human and machine intentions in a wide range of domains, which could open up exciting new avenues for research and development in this emerging field.

1.5 Notations and Assumptions

For any $x \in \mathbb{R}$, we define the sign operator as $\text{Sign}(x) = 1$ if $x \geq 0$ and -1 otherwise, and extend it to vectors by applying it element-wise. For a d -dimensional vector x , we denote the d -dimensional standard Gaussian distribution by $\mathcal{N}(0, I_d)$. The notation $|\mathcal{S}|$ refers to the number of elements in the set \mathcal{S} .

Assumption 1. *Throughout this paper, we have the following assumptions on the objective function f :*

1. f is twice continuously differentiable.
2. f is L -smooth, meaning that $\|\nabla^2 f(x)\| \leq L$.
3. f is lower bounded by a value f^* , that is, $f(x) \geq f^*$ for all x .

1.6 Paper organization

The rest of this paper is structured as follows: Section 2 introduces a novel approach for estimating descent direction based on ranking information, with a theoretical analysis of how different ranking oracles relate to the variance of the estimated direction. Built on the foundations in Section 2 and 2.2, Section 3 presents the main algorithm, ZO-RankSGD, along with the corresponding convergence analysis. In Section 4, we demonstrate the effectiveness of ZO-RankSGD through various experiments, ranging from synthetic data to real-world applications. Finally, Section 5 concludes the paper by summarizing our findings and suggesting future research directions.

2 Finding descent direction from the ranking information

2.1 A comparison-based estimator for descent direction

In contrast to the prior work [3], which relies on one-bit compressive sensing to recover the gradient, we propose a simple yet effective estimator for descent direction without requiring solving any compressive sensing problem. Given an objective function f and a point x , we estimate the descent direction of f using two independent Gaussian random vectors ξ_1 and ξ_2 as follows:

$$\hat{g}(x) = S_f(x, \xi_1, \xi_2, \mu)(\xi_1 - \xi_2), \quad (2)$$

where $\mu > 0$ is a constant, and $S_f(x, \xi_1, \xi_2, \mu) : \mathbb{R}^d \times \mathbb{R}^d \times \mathbb{R}^d \times \mathbb{R}_+ \rightarrow \{1, -1\}$ is defined as:

$$S_f(x, \xi_1, \xi_2, \mu) \stackrel{\text{def.}}{=} \text{Sign}((f(x + \mu\xi_1) - f(x + \mu\xi_2))). \quad (3)$$

We prove in Lemma 1, which is one of the most important technical tools in this work, that $\hat{g}(x)$ is an effective estimator for descent direction.

Lemma 1. *For any $x \in \mathbb{R}^d$, we have*

$$\langle \nabla f(x), \mathbb{E}[\hat{g}(x)] \rangle \geq \|\nabla f(x)\| - C_d \mu L, \quad (4)$$

where $C_d \geq 0$ is some constant that only depends on d .

Denote $\gamma > 0$ as the step size. From L -smoothness of f , we can show that

$$\begin{aligned} \mathbb{E}_{\xi_1, \xi_2} [f(x - \gamma\hat{g}(x))] - f(x) &\leq -\gamma \langle \nabla f(x), \mathbb{E}[\hat{g}(x)] \rangle + \frac{\gamma^2 L}{2} E[\|\hat{g}(x)\|^2] \\ &\leq -\gamma \|\nabla f(x)\| + \gamma C_d \mu L + \gamma^2 L d, \end{aligned} \quad (5)$$

where we use the equality $\mathbb{E}[\|\hat{g}(x)\|^2] = \mathbb{E}[\|\xi_1 - \xi_2\|^2] = 2d$. Therefore, whenever $\|\nabla f(x)\| \neq 0$, the value $\mathbb{E}_{\xi_1, \xi_2}[f(x - \gamma\hat{g}(x))]$ would be strictly smaller than $f(x)$ with sufficiently small γ and μ .

Besides, unlike the comparison-based gradient estimator proposed in [3], our estimator (2) can be directly incorporated with ranking oracles, as we will see in the next section.

2.2 From ranking information to pairwise comparison

We first observe that ranking information can be translated into pairwise comparisons. For instance, knowing that x_1 is the best among x_1, x_2, x_3 can be represented using two pairwise comparisons: x_1 is better than x_2 and x_1 is better than x_3 . Therefore, we propose to represent the input and output of (m, k) -ranking oracles as a directed acyclic graph (DAG), $\mathcal{G} = (\mathcal{N}, \mathcal{E})$, where the node set $\mathcal{N} = \{1, \dots, m\}$ and the directed edge set $\mathcal{E} = \{(i, j) \mid f(x_i) < f(x_j)\}$. An example of such a DAG is shown in Figure 2.

Given access to a (m, k) -ranking oracle $O_f^{(m, k)}$ and a starting point x , we can query $O_f^{(m, k)}$ with the inputs $x_i = x + \mu\xi_i$, $\xi_i \sim \mathcal{N}(0, I_d)$, for $i = 1, \dots, m$. With the DAG $\mathcal{G} = (\mathcal{N}, \mathcal{E})$ constructed from the ranking information of $O_f^{(m, k)}$, we propose the following rank-based gradient estimator:

$$\tilde{g}(x) = \frac{1}{|\mathcal{E}|} \sum_{(i, j) \in \mathcal{E}} \frac{x_j - x_i}{\mu} = \frac{1}{|\mathcal{E}|} \sum_{(i, j) \in \mathcal{E}} (\xi_j - \xi_i). \quad (6)$$

Remark 1. *Notice that (6) can be simply expressed as a linearly weighted combination of ξ_1, \dots, ξ_m . We provide the specific form in Appendix A.*

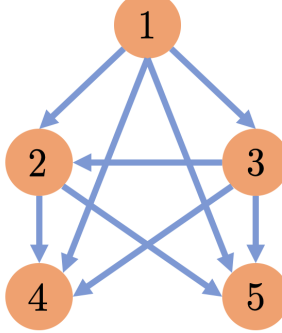


Figure 2: The corresponding DAG for the ranking result $O_f^{(5,3)}(x_1, x_2, x_3, x_4, x_5) = (1, 3, 2)$.

We note that (2) is a special case of (6) with $m = 2$ and $k = 1$, and it can be easily shown that $\mathbb{E}[\tilde{g}(x)] = \mathbb{E}[\hat{g}(x)]$ and $\mathbb{E}[|\tilde{g}(x)|^2] \leq \mathbb{E}[|\hat{g}(x)|^2]$, indicating that the benefit of using ranking information over a single comparison is a reduced variance of the gradient estimator. However, to determine the extent of variance reduction, we must examine the graph topology of \mathcal{G} .

Graph topology of \mathcal{G} . The construction of the DAG \mathcal{G} described above reveals that the graph topology of \mathcal{G} is uniquely determined by m and k . Especially, there are two important statistics of this graph topology.

The first statistic is the number of edges $|\mathcal{E}|$, which is related to the number of pairwise comparisons that can be extracted from the ranking result. In the precedent work [3], the number of pairwise comparisons was used to determine the variance of the gradient estimator. However, this is insufficient for our case, as the pairwise comparisons in (6) are not independent.

Therefore, we require the second statistic of the DAG, which is the number of neighboring edge pairs in \mathcal{E} . We define a neighboring edge pair as a pair of edges that share the same node. For instance, in Figure 2, one neighboring edge pair is (x_1, x_3) and (x_1, x_2) . We denote this number as $N(\mathcal{E})$ and define it formally as follows:

$$N(\mathcal{E}) \stackrel{\text{def}}{=} |\{((i, j), (i', j)) \in \bar{\mathcal{E}} \times \bar{\mathcal{E}} | i \neq i'\}|, \quad (7)$$

where $\bar{\mathcal{E}}$ is the undirected version of \mathcal{E} , namely, the edge (i, j) is equivalent to (j, i) in $\bar{\mathcal{E}}$.

As mentioned, the graph topology of \mathcal{G} is determined by m and k . Therefore, we can analytically compute $|\mathcal{E}|$ and $N(\mathcal{E})$ using m and k . We state these calculations in the following lemma:

Lemma 2. *Let $\mathcal{G} = (\mathcal{N}, \mathcal{E})$ be the DAG constructed from the ranking information of $O_f^{(m,k)}$, then we have:*

$$|\mathcal{E}| = km - (k^2 + k)/2, \quad (8)$$

$$N(\mathcal{E}) = m^2k + mk^2 - k^3 + k^2 - 4mk + 2k. \quad (9)$$

Variance analysis of (6) based on the graph topology. To analyze the variance of the estimator (6), we introduce two important metrics $M_1(f, \mu)$ and $M_2(f, \mu)$ on the function f .

Definition 2.

$$M_1(f, \mu) \stackrel{\text{def}}{=} \max_x \left\| \mathbb{E}_{\xi_1, \xi_2} [S_f(x, \xi_1, \xi_2, \mu)(\xi_1 - \xi_2)] \right\|^2, \quad (10)$$

$$M_2(f, \mu) \stackrel{\text{def}}{=} \max_x \mathbb{E}_{\xi_1, \xi_2, \xi_3} [S_f(x, \xi_1, \xi_2, \mu)S_f(x, \xi_1, \xi_3, \mu)\langle \xi_1 - \xi_2, \xi_1 - \xi_3 \rangle], \quad (11)$$

where ξ_1, ξ_2 and ξ_3 are three independent random vectors drawn from $\mathcal{N}(0, I_d)$.

Lemma 3 provides some useful upper bounds on $M_1(f, \mu)$ and $M_2(f, \mu)$, which help to understand the scale of these two quantities better.

Lemma 3. *For any function f and $\mu > 0$, we have $M_1(f, \mu) \leq 2d$, $M_2(f, \mu) \leq 2d$. Moreover, if f satisfies that $\nabla^2 f(x) = cI_d$ where $c \in \mathbb{R}$ is some constant, we have $M_1(f, \mu) \leq 32/\pi$.*

With $M_1(f, \mu)$ and $M_2(f, \mu)$, we can bound the second order moment of (6) as shown in the following Lemma 4.

Lemma 4. For any $x \in \mathbb{R}^d$, we have

$$\mathbb{E}[\|\tilde{g}(x)\|^2] \leq \frac{2d}{|\mathcal{E}|} + \frac{N(\mathcal{E})}{|\mathcal{E}|^2} M_2(f, \mu) + M_1(f, \mu). \quad (12)$$

Discussion on Lemma 4. With Lemma 2 and Lemma 3, we observe that the first variance term in (12), i.e., $\frac{2d}{|\mathcal{E}|}$, is $\mathcal{O}(\frac{1}{km})$, and thus vanishes as $m \rightarrow \infty$. In contrast, the second variance term $\frac{N(\mathcal{E})}{|\mathcal{E}|^2} M_2(f, \mu)$ does not disappear as m grows, because

$$\lim_{m \rightarrow \infty} \frac{N(\mathcal{E})}{|\mathcal{E}|^2} = \lim_{m \rightarrow \infty} \frac{m^2 k + m k^2 - k^3 + k^2 - 4 m k + 2 k}{(km - (k^2 + k)/2)^2} = \frac{1}{k}, \quad (13)$$

and thus only vanishes when both k and m tend to infinity. Finally, there is a non-diminishing term $M_1(f, \mu)$ remaining in (12). However, as shown in Lemma 3, $M_1(f, \mu)$ is smaller than $2d$ and can be bounded by a dimension-independent constant for a certain family of functions.

Remark 2. It is worth noting that our analysis can be simply extended to any ranking oracles beyond the (m, k) -ranking oracle. However, we only present the analysis for the (m, k) -ranking oracle in this work, as it is the common one in practice.

3 ZO-RankSGD: Zeroth-Order Rank-based Stochastic Gradient Descent

Now that we have presented all of our findings in Sections 2 and 2.2, we are prepared to introduce our proposed algorithm, ZO-RankSGD. The pseudocode for ZO-RankSGD is outlined in Algorithm 1, and it utilizes the gradient estimator (6) derived above.

Algorithm 1 ZO-RankSGD

Require: Initial point x_0 , stepsize η , number of iterations T , smoothing parameter μ , (m, k) -ranking oracle $O_f^{(m, k)}$.
1: **for** $t = 1$ to T **do**
2: Sample m i.i.d. random vectors $\{\xi_{(t,1)}, \dots, \xi_{(t,m)}\}$ from $N(0, I_d)$.
3: Query the (m, k) -ranking oracle $O_f^{(m, k)}$ with input $\{x_{t-1} + \mu \xi_{(t,1)}, \dots, x_{t-1} + \mu \xi_{(t,m)}\}$, and construct the corresponding DAG $\mathcal{G} = (\mathcal{N}, \mathcal{E})$ as described in Section 2.2.
4: Compute the gradient estimator using: $g_t = \frac{1}{|\mathcal{E}|} \sum_{(i,j) \in \mathcal{E}} (\xi_{(t,j)} - \xi_{(t,i)})$
5: $x_t = x_{t-1} - \eta g_t$.
6: **end for**

3.1 Theoretical guarantee of ZO-RankSGD

Now we present the convergence result of Algorithm 1 in the following Theorem 1.

Theorem 1. For any $\eta > 0$, $\mu > 0$, $T \in \mathbb{N}$, after running Algorithm 1 for T iterations, we have:

$$\mathbb{E} \left[\min_{t \in \{1, \dots, T\}} \|\nabla f(x_{t-1})\| \right] \leq \frac{f(x_0) - f^*}{\eta T} + C_d \mu L + \frac{\eta L}{2} \left(\frac{2d}{|\mathcal{E}|} + \frac{N(\mathcal{E})}{|\mathcal{E}|^2} M_2(f, \mu) + M_1(f, \mu) \right), \quad (14)$$

where C_d is some constant that only depends on d .

Corollary 1. By taking $\eta = \sqrt{\frac{1}{dT}}$ and $\mu = \sqrt{\frac{d}{C_d^2 T}}$ in Theorem 1, we have

$$\mathbb{E} \left[\min_{t \in \{1, \dots, T\}} \|\nabla f(x_{t-1})\| \right] = \mathcal{O} \left(\sqrt{\frac{d}{T}} \right). \quad (15)$$

Effect of m and k on the convergence speed of Algorithm 1. As we have discussed in Section 2.2, m and k affect the convergence speed through the variance of the gradient estimator. Specifically, in the upper bound of (14), we have $\frac{2d}{|\mathcal{E}|} + \frac{N(\mathcal{E})}{|\mathcal{E}|^2} M_2(f, \mu) = \mathcal{O}(\frac{d}{km} + \frac{d}{k})$.

3.2 Line search via ranking oracle

In this section, we discuss two potential issues that may arise when implementing Algorithm 1. Firstly, it can be cumbersome to manually tune the step size η required for each iteration. Secondly, it may be challenging for users to know whether the objective function is decreasing in each iteration as the function values are not accessible.

In order to address these challenges, we propose a simple and effective line search method that leverages the $(l, 1)$ -ranking oracle to determine the optimal step size for each iteration. The method involves querying the oracle with a set of inputs $\{x_{t-1}, x_{t-1} - \eta\gamma g_t, \dots, x_{t-1} - \eta\gamma^{l-1} g_t\}$, where $\gamma \in (0, 1)$ represents a scaling factor that controls the rate of step size reduction. By monitoring whether or not x_t is equal to x_{t-1} , users can observe the progress of Algorithm 1, while simultaneously selecting a suitable step size to achieve the best results.

It is worth noting that this line search technique is not unique to Algorithm 1 and can be applied to any gradient-based optimization algorithm, including those in [22, 3]. To reflect this, we present the proposed line search method as Algorithm 2, under the assumption that the gradient estimator g_t has already been computed.

Algorithm 2 Line search strategy for gradient-based optimization algorithms

Require: Initial point x_0 , stepsize η , number of iterations T , shrinking rate $\gamma \in (0, 1)$, number of trials l .

```

1: for  $t = 1$  to  $T$  do
2:   Compute the gradient estimator  $g_t$ .
3:    $x_t = \arg \min_{x \in \mathcal{X}_t} f(x)$ , where  $\mathcal{X}_t = \{x_{t-1}, x_{t-1} - \eta\gamma g_t, \dots, x_{t-1} - \eta\gamma^{l-1} g_t\}$ .
4: end for

```

4 Experiments

4.1 Simple functions

In this section, we present experimental results demonstrating the effectiveness of Algorithm 1 on two simple functions:

1. Quadratic function: $f(x) = \|x\|_2^2$, $x \in \mathbb{R}^{100}$.
2. Rosenbrock function: $f(x) = \sum_{i=1}^{99} ((1 - x_i)^2 + 100(x_{i+1} - x_i^2)^2)$, $x = [x_1, \dots, x_{100}]^\top \in \mathbb{R}^{100}$.

To demonstrate the effectiveness of our algorithm and verify our theoretical claims, we conduct two experiments, and all figures are obtained by averaging over 10 independent runs and are visualized in the form of mean \pm std.

(1) Comparing Algorithm 1 with existing algorithms. In this first experiment, we compare Algorithm 1 with the following algorithms in the existing literature:

1. ZO-SGD [22]: A zeroth-order optimization algorithm for valuing oracle.
2. SCBO [3]: A zeroth-order algorithm for pairwise comparing oracle.
3. GLD-Fast [11]: A direct search algorithm for top-1 oracle, namely, $(m, 1)$ -ranking oracle.
4. CMA-ES [19, 12]: A heuristic optimization algorithm for ranking oracle.

To ensure a meaningful comparison, we fix the number of queries $m = 15$ at each iteration for all algorithms. For gradient-based algorithms, ZO-SGD, SCBO, and our ZO-RankSGD, we use query points for gradient estimation and 5 points for the line search. In this experiment, we set $m = k$ for ZO-RankSGD, i.e. it can receive the full ranking information. Moreover, we tune the hyperparameters such as stepsize, smoothing parameter, and line search parameter via grid search for each algorithm, and the details are provided in Appendix C.1.

Our experiment results in Figure 3 on the two functions show that the gradient-based algorithm can outperform the direct search algorithm GLD-Fast and the heuristic algorithm CMA-ES. Besides, Algorithm 1 can outperform SCBO because the ranking oracle contains more information than the pairwise comparison oracle. Additionally, Algorithm 1 behaves similarly to ZO-SGD, indicating that the ranking oracle can be almost as informative as the valuing oracle for zeroth-order optimization.

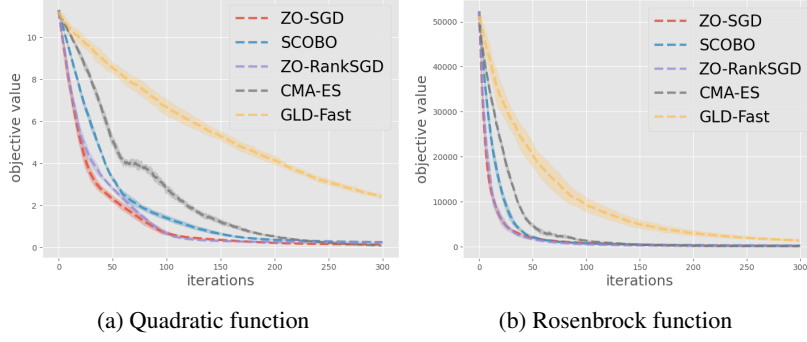


Figure 3: Performance of different algorithms.

(2) Investigating the impact of m and k on Algorithm 1. In this part, we aim to validate the findings presented in Lemma 4 and Theorem 1 by running Algorithm 1 with various values of m and k . To keep the setup simple, we set the step size η to 50 and the smoothing parameter μ to 0.01 for Algorithm 1 with line search (where $l = 5$ and $\gamma = 0.1$).

Figure 4 illustrates the performance of ZO-RankSGD under seven different combinations of m and k on the two functions. The results confirm our theoretical findings presented in Lemma 4. For example, we observe that $(m = 10, k = 10)$ yields better performance than $(m = 100, k = 1)$, as predicted by the second variance term in (12), which dominates and scales as $\mathcal{O}(\frac{1}{k})$.

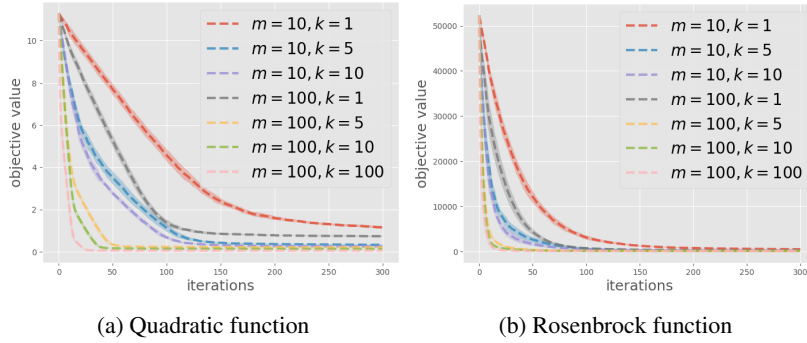


Figure 4: Performance of ZO-RankSGD under different combinations of m and k .

4.2 Reinforcement Learning with ranking oracle

Motivation. In this section, we consider the policy optimization problem in reinforcement learning with only a ranking oracle of the episode reward being available. Such a setting especially captures the scenario where human evaluators are asked to rank multiple episodes based on their expertise. In the existing RLHF approaches [24, 18, 23, 1], ranking feedback from humans is collected for every single action to train a reward model, and then the cumulative predicted reward is used as the performance measure for every episode. In contrast, the ranking feedback in our setting is collected directly on the episode level rather than the action level, providing a more precise evaluation of each episode’s performance.

We demonstrate the efficacy of ZO-RankSGD by showing that it can perform well on policy optimization described above. Specifically, we adopt a similar experimental setup as [3, 7], where the goal is to learn a policy for simulated robot control with several problems from the MuJoCo suite of benchmarks [35], and we restrict that the algorithm can only query the episode reward via a $(5, 5)$ -ranking oracle. We compare ZO-RankSGD to the CMA-ES algorithm, which is commonly used as a baseline in reinforcement learning [2] and also relies only on ranking oracle.

Results. The experiment results are shown in Figure 5, where the x-axis is the number of queries to the ranking oracle, and the y-axis is the ground-truth episode reward. In these experiments, we do not use line search for ZO-RankSGD, and instead, we let $\eta = \mu$, and decay them exponentially after every rollout. As can be seen from Figure 5, our algorithm can outperform CMA-ES by a significant margin on all three tasks, exhibiting a better ability to incorporate ranking information.

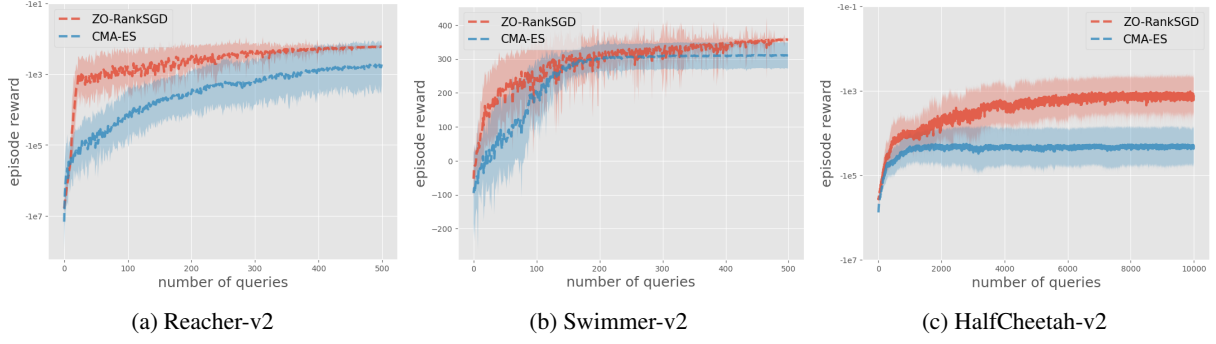


Figure 5: Performance of ZO-RankSGD and CMA-ES on three MuJoCo environments

4.3 Taming Diffusion Generative Model with Human Feedback

In recent years, there has been a growing interest in diffusion generative models, which have demonstrated remarkable performance in generating high-quality images [14, 31, 5]. However, these models often fall short of capturing fine details, such as human fingers. To address this issue, we draw inspiration from recent successes in aligning Language Models with human feedback [24, 18, 23, 1], and propose to utilize human ranking feedback to enhance the detail of the generated images.

We have noticed that there is a concurrent work [16] sharing a similar motivation with us. However, their method is still based on RLHF and requires a considerable amount of pre-collected data for fine-tuning the diffusion model. In contrast, our proposed method does not require any pre-collected data and does not need to fine-tune the diffusion model.

Experimental Setting. We focus on the task of text-to-image generation, using the state-of-the-art Stable Diffusion model [29] to generate images based on given text prompts. Our goal is to optimize the initial latent embedding using human ranking feedback through our proposed Algorithm 1, in order to produce images that are more appealing to humans. This experimental setting offers several advantages, including: (1) The latent embedding is a low-dimensional vector and thus requires far fewer rounds of human feedback compared to fine-tuning the entire model. (2) It can also serve as a data-collecting step before fine-tuning the model.

We note that any continuous parameter, such as the classifier-free guidance scale in the diffusion model, can be optimized using human feedback in a similar way. However, in this study, we focus solely on optimizing the latent embedding as we found that it is the most crucial factor for generating high-quality images.

Denoising diffusion process as a continuous mapping. Firstly, we remark that only ODE-based diffusion samplers, like DDIM [30] and DPM-solver [20], are used in this study as now the denoising diffusion process will be deterministic and only depends on the latent embedding. We demonstrate that optimizing the latent embedding is a valid continuous optimization problem by showing that, with slight perturbations of the latent embedding, diffusion samplers can usually generate multiple similar images. An example of this phenomenon is in Figure 6, where the first image is generated using a given latent embedding, while the next three images are generated by perturbing this embedding with noise drawn from $\mathcal{N}(0, 0.1I_d)$.

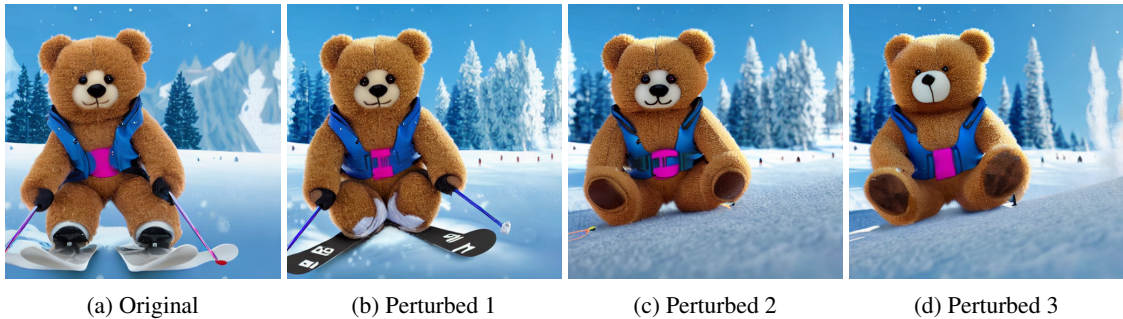


Figure 6: Continuous property of diffusion process. The used text prompt is *A teddy bear is skiing, detailed, realistic, 4K, 3D*.

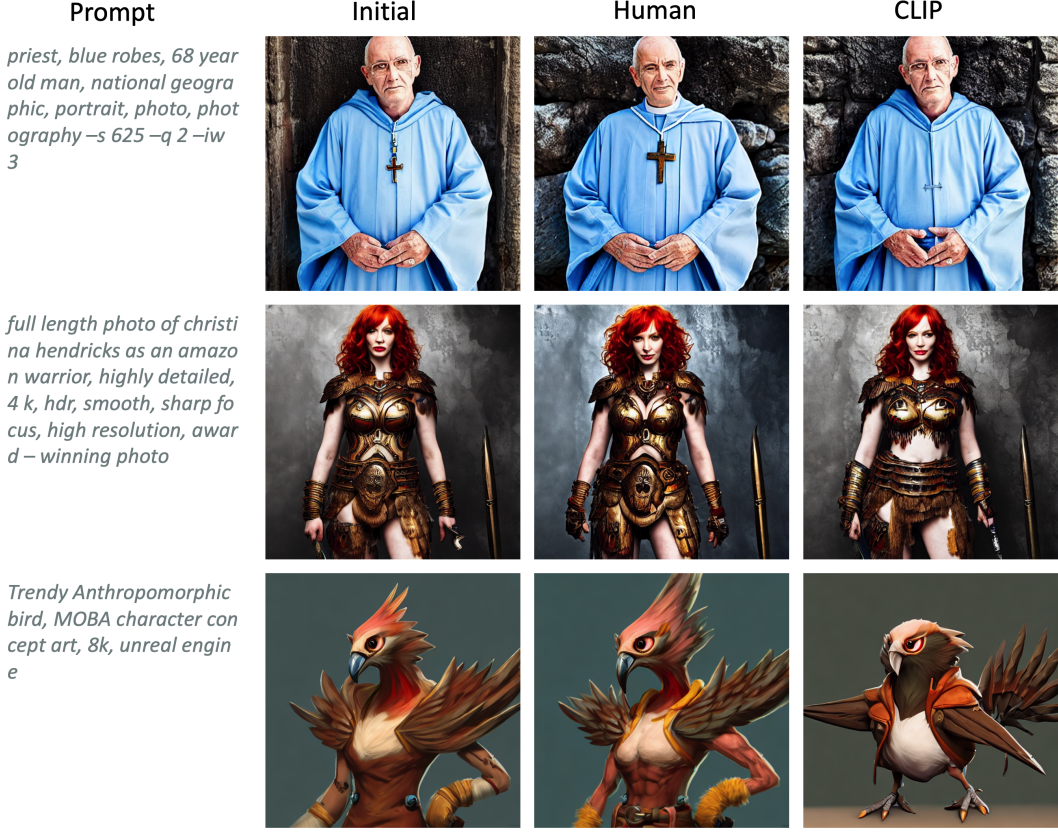


Figure 7: Examples of optimizing latent embedding in diffusion generative model. Initial: The initial images selected through multiple randomly generated latent embeddings serve as the initial points for the later optimization process. Human: The images obtained by optimizing human preference. CLIP: The images obtained by optimizing the CLIP similarity score [28].

Human feedback vs. CLIP score. The CLIP model [28], which is a state-of-the-art language and image contrastive model, can be used to determine the similarity between given texts and images. However, since the model is trained using noisy text-image pairs collected from the internet, it may not always perform well when details matter. In order to demonstrate the advantage of using human feedback, we compare the generated images obtained by optimizing human preference with those obtained by optimizing the CLIP similarity score [28].

Examples. We present some examples of optimization results in Figure 7. We use some popular text prompts from the internet¹ and provide human feedback ourselves in this experiment. As shown in the figure, our proposed Algorithm 1 can significantly improve the realism and detail of the generated images by leveraging human ranking feedback. Furthermore, we observe that those images obtained by optimizing the CLIP similarity score could produce worse images than the original ones, showing the necessity of human feedback.

For more examples like the ones in Figure 7, and the details of the entire optimization process, we refer the readers to Appendix C.2.

5 Conclusion

In conclusion, this paper rigorously studies a novel optimization problem where only a ranking oracle of the objective function is available. For this problem, we propose the first provable zeroth-order optimization algorithm, ZO-RankSGD, which has consistently demonstrated its efficacy across a wide range of applications. We also present how different ranking oracles can impact optimization performance, providing guidance on designing the user interface for ranking feedback.

¹<https://mpost.io/best-100-stable-diffusion-prompts-the-most-beautiful-ai-text-to-image-prompts>

Additionally, our algorithm has been shown to be a practical and effective way to incorporate human feedback, for example, it can be used to improve the detail of images generated by Stable Diffusion with human guidance. Furthermore, our approach, while can also be used for collecting data, offers a more efficient alternative to existing Reinforcement Learning with Human Feedback (RLHF) methods by enabling the online collection of ranking data and continuous improvement of model performance.

Possible future directions to this work may include extending the algorithm to handle noise and uncertainty in the ranking feedback, combining ZO-RankSGD with a model-based approach like Bayesian Optimization [10] to further improve the query efficiency, and applying it to other scenarios beyond human feedback.

References

- [1] Yuntao Bai, Andy Jones, Kamal Ndousse, Amanda Askell, Anna Chen, Nova DasSarma, Dawn Drain, Stanislav Fort, Deep Ganguli, Tom Henighan, et al. Training a helpful and harmless assistant with reinforcement learning from human feedback. *arXiv preprint arXiv:2204.05862*, 2022.
- [2] Viktor Bengs, Róbert Busa-Fekete, Adil El Mesaoudi-Paul, and Eyke Hüllermeier. Preference-based online learning with dueling bandits: A survey. *J. Mach. Learn. Res.*, 22:7–1, 2021.
- [3] HanQin Cai, Daniel Mckenzie, Wotao Yin, and Zhenliang Zhang. A one-bit, comparison-based gradient estimator. *Applied and Computational Harmonic Analysis*, 60:242–266, 2022.
- [4] Zhongxiang Dai, Bryan Kian Hsiang Low, and Patrick Jaillet. Differentially private federated bayesian optimization with distributed exploration. *Advances in Neural Information Processing Systems*, 34:9125–9139, 2021.
- [5] Prafulla Dhariwal and Alexander Nichol. Diffusion models beat gans on image synthesis. *Advances in Neural Information Processing Systems*, 34:8780–8794, 2021.
- [6] Jinshuo Dong, Aaron Roth, and Weijie Su. Gaussian differential privacy. *Journal of the Royal Statistical Society*, 2021.
- [7] Yan Duan, Xi Chen, Rein Houthooft, John Schulman, and Pieter Abbeel. Benchmarking deep reinforcement learning for continuous control. In *International conference on machine learning*, pages 1329–1338. PMLR, 2016.
- [8] John C Duchi, Michael I Jordan, Martin J Wainwright, and Andre Wibisono. Optimal rates for zero-order convex optimization: The power of two function evaluations. *IEEE Transactions on Information Theory*, 61(5):2788–2806, 2015.
- [9] Cynthia Dwork, Aaron Roth, et al. The algorithmic foundations of differential privacy. *Found. Trends Theor. Comput. Sci.*, 9(3-4):211–407, 2014.
- [10] Peter I Frazier. A tutorial on bayesian optimization. *arXiv preprint arXiv:1807.02811*, 2018.
- [11] Daniel Golovin, John Karro, Greg Kochanski, Chansoo Lee, Xingyou Song, and Qiuyi Zhang. Gradientless descent: High-dimensional zeroth-order optimization. *arXiv preprint arXiv:1911.06317*, 2019.
- [12] Nikolaus Hansen, Youhei Akimoto, and Petr Baudis. CMA-ES/pycma on Github. Zenodo, DOI:10.5281/zenodo.2559634, February 2019.
- [13] Filip Hanzely, Konstantin Mishchenko, and Peter Richtárik. Sega: Variance reduction via gradient sketching. *Advances in Neural Information Processing Systems*, 31, 2018.
- [14] Jonathan Ho, Ajay Jain, and Pieter Abbeel. Denoising diffusion probabilistic models. *Advances in Neural Information Processing Systems*, 33:6840–6851, 2020.
- [15] Ralph L Keeney and Howard Raiffa. *Decisions with multiple objectives: preferences and value trade-offs*. Cambridge university press, 1993.
- [16] Kimin Lee, Hao Liu, Moonkyung Ryu, Olivia Watkins, Yuqing Du, Craig Boutilier, Pieter Abbeel, Mohammad Ghavamzadeh, and Shixiang Shane Gu. Aligning text-to-image models using human feedback. *arXiv preprint arXiv:2302.12192*, 2023.
- [17] Lisha Li, Kevin Jamieson, Giulia DeSalvo, Afshin Rostamizadeh, and Ameet Talwalkar. Hyperband: A novel bandit-based approach to hyperparameter optimization. *The Journal of Machine Learning Research*, 18(1):6765–6816, 2017.
- [18] Hao Liu, Carmelo Sferrazza, and Pieter Abbeel. Languages are rewards: Hindsight finetuning using human feedback, 2023.

[19] Ilya Loshchilov and Frank Hutter. Cma-es for hyperparameter optimization of deep neural networks. *arXiv preprint arXiv:1604.07269*, 2016.

[20] Cheng Lu, Yuhao Zhou, Fan Bao, Jianfei Chen, Chongxuan Li, and Jun Zhu. Dpm-solver: A fast ode solver for diffusion probabilistic model sampling in around 10 steps. *arXiv preprint arXiv:2206.00927*, 2022.

[21] John A Nelder and Roger Mead. A simplex method for function minimization. *The computer journal*, 7(4):308–313, 1965.

[22] Yurii Nesterov and Vladimir Spokoiny. Random gradient-free minimization of convex functions. *Foundations of Computational Mathematics*, 17(2):527–566, 2017.

[23] OpenAI. Chatgpt, <https://openai.com/blog/chatgpt/>, 2022.

[24] Long Ouyang, Jeff Wu, Xu Jiang, Diogo Almeida, Carroll L Wainwright, Pamela Mishkin, Chong Zhang, Sandhini Agarwal, Katarina Slama, Alex Ray, et al. Training language models to follow instructions with human feedback. *arXiv preprint arXiv:2203.02155*, 2022.

[25] Yaniv Plan and Roman Vershynin. Robust 1-bit compressed sensing and sparse logistic regression: A convex programming approach. *IEEE Transactions on Information Theory*, 59(1):482–494, 2012.

[26] Michael JD Powell. Direct search algorithms for optimization calculations. *Acta numerica*, 7:287–336, 1998.

[27] Gang Qiao, Weijie Su, and Li Zhang. Oneshot differentially private top-k selection. In *International Conference on Machine Learning*, pages 8672–8681. PMLR, 2021.

[28] Alec Radford, Jong Wook Kim, Chris Hallacy, Aditya Ramesh, Gabriel Goh, Sandhini Agarwal, Girish Sastry, Amanda Askell, Pamela Mishkin, Jack Clark, et al. Learning transferable visual models from natural language supervision. In *International conference on machine learning*, pages 8748–8763. PMLR, 2021.

[29] Robin Rombach, Andreas Blattmann, Dominik Lorenz, Patrick Esser, and Björn Ommer. High-resolution image synthesis with latent diffusion models. In *Proceedings of the IEEE/CVF Conference on Computer Vision and Pattern Recognition*, pages 10684–10695, 2022.

[30] Jiaming Song, Chenlin Meng, and Stefano Ermon. Denoising diffusion implicit models. *arXiv preprint arXiv:2010.02502*, 2020.

[31] Yang Song, Jascha Sohl-Dickstein, Diederik P Kingma, Abhishek Kumar, Stefano Ermon, and Ben Poole. Score-based generative modeling through stochastic differential equations. *arXiv preprint arXiv:2011.13456*, 2020.

[32] Nisan Stiennon, Long Ouyang, Jeffrey Wu, Daniel Ziegler, Ryan Lowe, Chelsea Voss, Alec Radford, Dario Amodei, and Paul F Christiano. Learning to summarize with human feedback. *Advances in Neural Information Processing Systems*, 33:3008–3021, 2020.

[33] Zhiwei Tang, Tsung-Hui Chang, Xiaojing Ye, and Hongyuan Zha. Low-rank matrix recovery with unknown correspondence. *arXiv preprint arXiv:2110.07959*, 2021.

[34] Zhiwei Tang, Yanmeng Wang, and Tsung-Hui Chang. \$z\$-signfedavg: A unified sign-based stochastic compression for federated learning. In *Workshop on Federated Learning: Recent Advances and New Challenges (in Conjunction with NeurIPS 2022)*, 2022.

[35] Emanuel Todorov, Tom Erez, and Yuval Tassa. Mujoco: A physics engine for model-based control. In *2012 IEEE/RSJ international conference on intelligent robots and systems*, pages 5026–5033. IEEE, 2012.

[36] Yuxin Wen, Neel Jain, John Kirchenbauer, Micah Goldblum, Jonas Geiping, and Tom Goldstein. Hard prompts made easy: Gradient-based discrete optimization for prompt tuning and discovery. *arXiv preprint arXiv:2302.03668*, 2023.

[37] Kai Zheng, Tianle Cai, Weiran Huang, Zhenguo Li, and Liwei Wang. Locally differentially private (contextual) bandits learning. *Advances in Neural Information Processing Systems*, 33:12300–12310, 2020.

[38] Xingyu Zhou and Jian Tan. Local differential privacy for bayesian optimization. In *Proceedings of the AAAI Conference on Artificial Intelligence*, volume 35, pages 11152–11159, 2021.

Appendix

A A simplified expression for (6)

Let $\mathcal{G} = (\mathcal{N}, \mathcal{E})$ be the DAG constructed from the ranking information of $O_f^{(m,k)}$, we denote the input degrees and output degrees of $x_i \in \mathcal{N}$ as $\deg_{\text{in}}(i)$ and $\deg_{\text{out}}(i)$ respectively. We first notice that

$$\sum_{(i,j) \in \mathcal{E}} (\xi_j - \xi_i) = \sum_{i=1}^m (\deg_{\text{in}}(i) - \deg_{\text{out}}(i)) \xi_i. \quad (16)$$

Denote $w_i = \deg_{\text{in}}(i) - \deg_{\text{out}}(i)$, if $O_f^{(m,k)}(x_1, \dots, x_m) = (i_1, \dots, i_k)$, then we can compute that

$$w_{i_j} = \deg_{\text{in}}(i_j) - \deg_{\text{out}}(i_j) = j - 1 - (m - j) = 2j - m - 1, \quad j = 1, \dots, k. \quad (17)$$

$$w_q = \deg_{\text{in}}(q) - \deg_{\text{out}}(q) = k - 0 = k, \quad q \notin \{i_1, \dots, i_k\}. \quad (18)$$

B Missing Proof

Proof of Lemma 1. In the following proof, we denote $p(\cdot)$ as the pdf function of $\mathcal{N}(0, I_d)$ for arbitrary dimension d .

We first rewrite $\langle \nabla f(x), \hat{g}(x) \rangle$ as follows:

$$\langle \nabla f(x), \hat{g}(x) \rangle = \langle \nabla f(x), S_f(x, \xi_1, \xi_2, \mu)(\xi_1 - \xi_2) \rangle = S_f(x, \xi_1, \xi_2, \mu) \cdot \langle \nabla f(x), \xi_1 - \xi_2 \rangle. \quad (19)$$

By the second-order Taylor expansion with Cauchy remainders, we notice that

$$f(x + \mu \xi_1) = f(x) + \mu \langle \nabla f(x), \xi_1 \rangle + \frac{\mu^2}{2} \xi_1^\top \nabla^2 f(x_1) \xi_1, \quad (20)$$

$$f(x + \mu \xi_2) = f(x) + \mu \langle \nabla f(x), \xi_2 \rangle + \frac{\mu^2}{2} \xi_2^\top \nabla^2 f(x_2) \xi_2, \quad (21)$$

where x_1 and x_2 are two points around x .

With (20) and (21) we can write $S_f(x, \xi_1, \xi_2, \mu)$ as follows:

$$S_f(x, \xi_1, \xi_2, \mu) = \text{Sign} \left(\langle \nabla f(x), \xi_1 - \xi_2 \rangle + \frac{\mu}{2} \xi_1^\top \nabla^2 f(x_1) \xi_1 - \frac{\mu}{2} \xi_2^\top \nabla^2 f(x_2) \xi_2 \right). \quad (22)$$

Now we start to bound the term

$$\mathbb{E} [S_f(x, \xi_1, \xi_2, \mu) \cdot \langle \nabla f(x), \xi_1 - \xi_2 \rangle], \quad (23)$$

where the expectation is taken over the random direction ξ_1 and ξ_2 .

Before doing that, we first define two important regions:

$$\mathcal{R}_1 = \{(\xi_1, \xi_2) \mid \langle \nabla f(x), \xi_1 - \xi_2 \rangle > 0\}, \quad (24)$$

$$\mathcal{R}_{11} = \{(\xi_1, \xi_2) \mid (\xi_1, \xi_2) \in \mathcal{R}_1, S_f(x, \xi_1, \xi_2, \mu) \neq \text{Sign}(\langle \nabla f(x), \xi_1 - \xi_2 \rangle)\}. \quad (25)$$

Notice that when $(\xi_1, \xi_2) \in \mathcal{R}_1$, $S_f(x, \xi_1, \xi_2, \mu) \neq \text{Sign}(\langle \nabla f(x), \xi_1 - \xi_2 \rangle)$ is equivalent to

$$\langle \nabla f(x), \xi_1 - \xi_2 \rangle + \frac{\mu}{2} \xi_1^\top \nabla^2 f(x_1) \xi_1 - \frac{\mu}{2} \xi_2^\top \nabla^2 f(x_2) \xi_2 < 0.$$

Also, from L -smoothness, we can know that

$$-\frac{\mu L}{2} (\|\xi_1\|_2^2 + \|\xi_2\|_2^2) \leq \frac{\mu}{2} \xi_1^\top \nabla^2 f(x_1) \xi_1 - \frac{\mu}{2} \xi_2^\top \nabla^2 f(x_2) \xi_2.$$

We denote the region

$$\bar{\mathcal{R}}_{11} = \{(\xi_1, \xi_2) \mid (\xi_1, \xi_2) \in \mathcal{R}_1, \langle \nabla f(x), \xi_1 - \xi_2 \rangle - \frac{\mu L}{2} (\|\xi_1\|_2^2 + \|\xi_2\|_2^2) < 0\}. \quad (26)$$

It is easy to verify that $\mathcal{R}_{11} \subseteq \bar{\mathcal{R}}_{11}$. Let $\mathcal{R}_{12} = \mathcal{R}_1 \setminus \bar{\mathcal{R}}_{11}$, we can have the following inequality.

$$\int_{\mathcal{R}_1} S_f(x, \xi_1, \xi_2, \mu) \langle \nabla f(x), \xi_1 - \xi_2 \rangle p(\xi_1) p(\xi_2) d\xi_1 d\xi_2 \quad (27)$$

$$\begin{aligned} &= \int_{\mathcal{R}_1 / \mathcal{R}_{11}} S_f(x, \xi_1, \xi_2, \mu) \langle \nabla f(x), \xi_1 - \xi_2 \rangle p(\xi_1) p(\xi_2) d\xi_1 d\xi_2 \\ &\quad + \int_{\mathcal{R}_{11}} S_f(x, \xi_1, \xi_2, \mu) \langle \nabla f(x), \xi_1 - \xi_2 \rangle p(\xi_1) p(\xi_2) d\xi_1 d\xi_2 \end{aligned} \quad (28)$$

$$\begin{aligned} &= \int_{\mathcal{R}_1 / \mathcal{R}_{11}} \langle \nabla f(x), \xi_1 - \xi_2 \rangle p(\xi_1) p(\xi_2) d\xi_1 d\xi_2 \\ &\quad - \int_{\mathcal{R}_{11}} \langle \nabla f(x), \xi_1 - \xi_2 \rangle p(\xi_1) p(\xi_2) d\xi_1 d\xi_2 \end{aligned} \quad (29)$$

$$\begin{aligned} &\geq \int_{\mathcal{R}_1 / \bar{\mathcal{R}}_{11}} \langle \nabla f(x), \xi_1 - \xi_2 \rangle p(\xi_1) p(\xi_2) d\xi_1 d\xi_2 \\ &\quad - \int_{\mathcal{R}_{11}} \langle \nabla f(x), \xi_1 - \xi_2 \rangle p(\xi_1) p(\xi_2) d\xi_1 d\xi_2 \end{aligned} \quad (30)$$

$$\begin{aligned} &= 2 \int_{\mathcal{R}_{12}} \langle \nabla f(x), \xi_1 - \xi_2 \rangle p(\xi_1) p(\xi_2) d\xi_1 d\xi_2 \\ &\quad - \int_{\mathcal{R}_1} \langle \nabla f(x), \xi_1 - \xi_2 \rangle p(\xi_1) p(\xi_2) d\xi_1 d\xi_2. \end{aligned} \quad (31)$$

Before we proceed to study the property of the integral in (31), let us first define an important function. Consider the function $h(v, r, d) : \mathbb{R} \times \mathbb{R}_+ \times \mathbb{Z}_+ \rightarrow \mathbb{R}$ defined as follows:

$$h(v, r, d) \stackrel{\text{def.}}{=} \sqrt{2}v \int_0^{\frac{2\sqrt{2}v}{r}} x F_{2d-1} \left(\left(\frac{2\sqrt{2}v}{r} - x \right) x \right) p(x) dx, \quad (32)$$

where $F_{2d-1}(\cdot)$ is the CDF of the χ^2 distribution with $2d - 1$ degrees of freedom. With this function, we can have the following lemma that presents the close form of the integrals in (31).

Lemma 5.

$$\int_{\mathcal{R}_1} \langle \nabla f(x), \xi_1 - \xi_2 \rangle p(\xi_1) p(\xi_2) d\xi_1 d\xi_2 = \frac{1}{\sqrt{\pi}} \|\nabla f(x)\|, \quad (33)$$

$$\int_{\mathcal{R}_{12}} \langle \nabla f(x), \xi_1 - \xi_2 \rangle p(\xi_1) p(\xi_2) d\xi_1 d\xi_2 = h(\|\nabla f(x)\|, \mu L, d). \quad (34)$$

Also, we need an important lemma on $h(v, r, d)$.

Lemma 6. For any $d \in \mathbb{Z}_+$, there exist a constant $C_d > 0$ such that for any $v \geq 0, r > 0$,

$$h(v, r, d) \geq \left(\frac{1}{2\sqrt{\pi}} + \frac{1}{4} \right) v - \frac{1}{4} C_d r. \quad (35)$$

Combining (31), (33), (34) and (35), we have

$$\int_{\mathcal{R}_1} S_f(x, \xi_1, \xi_2, \mu) \langle \nabla f(x), \xi_1 - \xi_2 \rangle p(\xi_1) p(\xi_2) d\xi_1 d\xi_2 \geq \frac{1}{2} \|\nabla f(x)\| - \frac{1}{2} C_d \mu L. \quad (36)$$

Similarly, if we define

$$\mathcal{R}_2 = \{(\xi_1, \xi_2) \mid \langle \nabla f(x), \xi_1 - \xi_2 \rangle < 0\},$$

we have

$$\int_{\mathcal{R}_2} S_f(x, \xi_1, \xi_2, \mu) \langle \nabla f(x), \xi_1 - \xi_2 \rangle p(\xi_1)p(\xi_2) d\xi_1 d\xi_2 \quad (37)$$

$$= \int_{\mathcal{R}_2} S_f(x, \xi_2, \xi_1, \mu) \langle \nabla f(x), \xi_2 - \xi_1 \rangle p(\xi_1)p(\xi_2) d\xi_1 d\xi_2 \quad (38)$$

$$= \int_{\mathcal{R}_1} S_f(x, \xi_1, \xi_2, \mu) \langle \nabla f(x), \xi_1 - \xi_2 \rangle p(\xi_1)p(\xi_2) d\xi_1 d\xi_2, \quad (39)$$

because the integral on \mathcal{R}_1 is symmetric to the integral on \mathcal{R}_2 by swapping ξ_1 and ξ_2 . Since $\mathbb{R}^{2d}/(\mathcal{R}_1 \cup \mathcal{R}_2)$ has zero measure, we have

$$\mathbb{E} [S_f(x, \xi_1, \xi_2, \mu) \cdot \langle \nabla f(x), \xi_1 - \xi_2 \rangle] = 2 \int_{\mathcal{R}_1} \langle \nabla f(x), \xi_2 - \xi_1 \rangle p(\xi_1)p(\xi_2) d\xi_1 d\xi_2 \quad (40)$$

$$\geq \|\nabla f(x)\| - C_d \mu L. \quad (41)$$

□

Proof of Lemma 2. Suppose that $O_f^{(m,k)}(x_1, \dots, x_m) = (i_1, \dots, i_k)$, we separate \mathcal{N} into two node sets:

$$\mathcal{N}_1 = \{i_1, \dots, i_k\} \text{ and } \mathcal{N}_2 = \{q \in \{1, \dots, m\} \mid q \notin \{i_1, \dots, i_k\}\}.$$

Firstly, since the subgraph of \mathcal{G} on \mathcal{N}_1 is a complete graph, the number of edges in this subgraph is $k(k-1)/2$. The remaining edges in \mathcal{G} connect the node in \mathcal{N}_2 to the node in \mathcal{N}_1 , hence the number of them is $k(m-k)$. Therefore,

$$|\mathcal{E}| = k(k-1)/2 + k(m-k) = km - (k^2 + k)/2. \quad (42)$$

Now we denote the set of neighboring edge pairs as $\mathcal{S} = \{((i, j), (i', j)) \in \bar{\mathcal{E}} \times \bar{\mathcal{E}} \mid i \neq i'\}$. We can split \mathcal{S} as the following five set:

$$S_1 = \{((i, j), (i', j)) \in \bar{\mathcal{E}} \times \bar{\mathcal{E}} \mid i \neq i', i \in \mathcal{N}_1, i' \in \mathcal{N}_1, j \in \mathcal{N}_1\}, \quad (43)$$

$$S_2 = \{((i, j), (i', j)) \in \bar{\mathcal{E}} \times \bar{\mathcal{E}} \mid i \neq i', i \in \mathcal{N}_1, i' \in \mathcal{N}_1, j \in \mathcal{N}_2\}, \quad (44)$$

$$S_3 = \{((i, j), (i', j)) \in \bar{\mathcal{E}} \times \bar{\mathcal{E}} \mid i \neq i', i \in \mathcal{N}_1, i' \in \mathcal{N}_2, j \in \mathcal{N}_1\}, \quad (45)$$

$$S_4 = \{((i, j), (i', j)) \in \bar{\mathcal{E}} \times \bar{\mathcal{E}} \mid i \neq i', i \in \mathcal{N}_2, i' \in \mathcal{N}_1, j \in \mathcal{N}_1\}, \quad (46)$$

$$S_5 = \{((i, j), (i', j)) \in \bar{\mathcal{E}} \times \bar{\mathcal{E}} \mid i \neq i', i \in \mathcal{N}_2, i' \in \mathcal{N}_2, j \in \mathcal{N}_1\}. \quad (47)$$

For the first set \mathcal{S}_1 , we can compute that

$$|\mathcal{S}_1| = 6 \binom{k}{3} = k(k-1)(k-2), \quad (48)$$

because every edge pair composes of three nodes, and every three nodes can form 6 edge pairs.

For the second set \mathcal{S}_2 , we have

$$|\mathcal{S}_2| = 2(m-k) \binom{k}{2} = (m-k)k(k-1), \quad (49)$$

because $|\mathcal{N}_2| = m-k$ and $|\{(i, i') \in \mathcal{N}_1 \times \mathcal{N}_1 \mid i \neq i'\}| = 2 \binom{k}{2}$.

Similarly, for the set \mathcal{S}_3 and \mathcal{S}_4 , we can obtain

$$|\mathcal{S}_3| = |\mathcal{S}_4| = 2(m-k) \binom{k}{2} = (m-k)k(k-1). \quad (50)$$

Finally, for the set \mathcal{S}_5 , we can compute that

$$|\mathcal{S}_5| = 2k \binom{m-k}{2} = k(m-k)(m-k-1), \quad (51)$$

because $|\mathcal{N}_1| = k$ and $|\{(i, i') \in \mathcal{N}_2 \times \mathcal{N}_2 \mid i \neq i'\}| = 2 \binom{m-k}{2}$.

In all, we have

$$|\mathcal{S}| = |\mathcal{S}_1| + |\mathcal{S}_2| + |\mathcal{S}_3| + |\mathcal{S}_4| + |\mathcal{S}_5| \quad (52)$$

$$= k(k-1)(k-2) + 3(m-k)k(k-1) + k(m-k)(m-k-1) \quad (53)$$

$$= m^2k + mk^2 - k^3 + k^2 - 4mk + 2k. \quad (54)$$

□

Proof of Lemma 3. We first prove that $M_1(f, \mu) \leq 2d$. From convexity of $\|\cdot\|^2$ and Jensen's inequality, we have

$$\left\| \mathbb{E}_{\xi_1, \xi_2} [S_f(x, \xi_1, \xi_2, \mu)(\xi_1 - \xi_2)] \right\|^2 \leq \mathbb{E}_{\xi_1, \xi_2} \| [S_f(x, \xi_1, \xi_2, \mu)(\xi_1 - \xi_2)] \|^2 = 2d. \quad (55)$$

Then we prove $M_2(f, \mu) \leq 2d$. From Cauchy-Schwarz inequality, we have

$$\mathbb{E}_{\xi_1, \xi_2, \xi_3} [S_f(x, \xi_1, \xi_2, \mu) S_f(x, \xi_1, \xi_3, \mu) \langle \xi_1 - \xi_2, \xi_1 - \xi_3 \rangle] \quad (56)$$

$$\leq \sqrt{\mathbb{E}_{\xi_1, \xi_2} [\|\xi_1 - \xi_2\|^2] \mathbb{E}_{\xi_1, \xi_3} [\|\xi_1 - \xi_3\|^2]} = 2d. \quad (57)$$

Now we study the mean vector $\mathbb{E}_{\xi_1, \xi_2} [S_f(x, \xi_1, \xi_2, \mu)(\xi_1 - \xi_2)]$ under the condition $\nabla^2 f(x) = cI_d$. We first write it as a sum of three vectors.

$$\mathbb{E}_{\xi_1, \xi_2} [S_f(x, \xi_1, \xi_2, \mu)(\xi_1 - \xi_2)] = \int_{f(x+\mu\xi_1) > f(x+\mu\xi_2)} (\xi_1 - \xi_2) p(\xi_1) p(\xi_2) d\xi_1 d\xi_2 \quad (58)$$

$$+ \int_{f(x+\mu\xi_1) = f(x+\mu\xi_2)} (\xi_1 - \xi_2) p(\xi_1) p(\xi_2) d\xi_1 d\xi_2 \quad (59)$$

$$+ \int_{f(x+\mu\xi_1) < f(x+\mu\xi_2)} (\xi_2 - \xi_1) p(\xi_1) p(\xi_2) d\xi_1 d\xi_2. \quad (60)$$

For the three vectors, we have

$$\int_{f(x+\mu\xi_1) = f(x+\mu\xi_2)} (\xi_1 - \xi_2) p(\xi_1) p(\xi_2) d\xi_1 d\xi_2 \quad (61)$$

$$= \int_{f(x+\mu\xi_1) = f(x+\mu\xi_2)} \xi_1 p(\xi_1) p(\xi_2) d\xi_1 d\xi_2 - \int_{f(x+\mu\xi_1) = f(x+\mu\xi_2)} \xi_2 p(\xi_1) p(\xi_2) d\xi_1 d\xi_2 \quad (62)$$

$$= 0, \quad (63)$$

and

$$\int_{f(x+\mu\xi_1) > f(x+\mu\xi_2)} (\xi_1 - \xi_2) p(\xi_1) p(\xi_2) d\xi_1 d\xi_2 \quad (64)$$

$$= \int_{f(x+\mu\xi_2) > f(x+\mu\xi_1)} (\xi_2 - \xi_1) p(\xi_1) p(\xi_2) d\xi_1 d\xi_2 \quad (65)$$

$$= \int_{f(x+\mu\xi_1) < f(x+\mu\xi_2)} (\xi_2 - \xi_1) p(\xi_1) p(\xi_2) d\xi_1 d\xi_2. \quad (66)$$

Therefore, we can write $\mathbb{E}_{\xi_1, \xi_2} [S_f(x, \xi_1, \xi_2, \mu)(\xi_1 - \xi_2)]$ as

$$\mathbb{E}_{\xi_1, \xi_2} [S_f(x, \xi_1, \xi_2, \mu)(\xi_1 - \xi_2)] = 2 \int_{f(x+\mu\xi_1) > f(x+\mu\xi_2)} (\xi_1 - \xi_2) p(\xi_1) p(\xi_2) d\xi_1 d\xi_2. \quad (67)$$

Now we study the integrals $\int_{f(x+\mu\xi_1) > f(x+\mu\xi_2)} \xi_1 p(\xi_1) p(\xi_2) d\xi_1 d\xi_2$ and $\int_{f(x+\mu\xi_1) > f(x+\mu\xi_2)} \xi_2 p(\xi_1) p(\xi_2) d\xi_1 d\xi_2$. We can compute that

$$\int_{f(x+\mu\xi_1) > f(x+\mu\xi_2)} \xi_1 p(\xi_1) p(\xi_2) d\xi_1 d\xi_2 \quad (68)$$

$$= \int_{\mathbb{R}^d} \left(\int_{f(x+\mu\xi_1) > f(x+\mu\xi_2)} p(\xi_2) d\xi_2 \right) \xi_1 p(\xi_1) d\xi_1, \quad (69)$$

and,

$$\int_{f(x+\mu\xi_1) > f(x+\mu\xi_2)} \xi_2 p(\xi_1) p(\xi_2) d\xi_1 d\xi_2 \quad (70)$$

$$= \int_{\mathbb{R}^d} \left(\int_{f(x+\mu\xi_1) > f(x+\mu\xi_2)} p(\xi_1) d\xi_1 \right) \xi_2 p(\xi_2) d\xi_2 \quad (71)$$

$$= \int_{\mathbb{R}^d} \left(\int_{f(x+\mu\xi_2) > f(x+\mu\xi_1)} p(\xi_2) d\xi_2 \right) \xi_1 p(\xi_1) d\xi_1 \quad (72)$$

The condition $\nabla^2 f(x) = cI_d$ implies that f is a quadratic function. We denote $\mathcal{M}(\cdot)$ as the Lebesgue measure on \mathbb{R}^d . Notice that $\mathcal{M}(\{\xi_2 \mid f(x+\mu\xi_2) = f(x+\mu\xi_1)\}) = 0$ because it is known that the zero point set of any polynomial function has zero Lebesgue measure. Therefore, we have

$$\int_{f(x+\mu\xi_1) > f(x+\mu\xi_2)} p(\xi_2) d\xi_2 + \int_{f(x+\mu\xi_2) > f(x+\mu\xi_1)} p(\xi_2) d\xi_2 \quad (73)$$

$$= 1 - \int_{f(x+\mu\xi_2) = f(x+\mu\xi_1)} p(\xi_2) d\xi_2 = 1. \quad (74)$$

Hence we have

$$\int_{f(x+\mu\xi_1) > f(x+\mu\xi_2)} (\xi_1 - \xi_2) p(\xi_1) p(\xi_2) d\xi_1 d\xi_2 \quad (75)$$

$$= 2 \int_{\mathbb{R}^d} \left(\int_{f(x+\mu\xi_1) > f(x+\mu\xi_2)} p(\xi_2) d\xi_2 \right) \xi_1 p(\xi_1) d\xi_1 - \int_{\mathbb{R}^d} \xi_1 p(\xi_1) d\xi_1 \quad (76)$$

$$= 2 \int_{\mathbb{R}^d} \left(\int_{f(x+\mu\xi_1) > f(x+\mu\xi_2)} p(\xi_2) d\xi_2 \right) \xi_1 p(\xi_1) d\xi_1. \quad (77)$$

Since $\nabla^2 f(x) = cI_d$, we have

$$f(x + \mu\xi_1) = f(x) + \mu \nabla f(x)^T \xi_1 + \frac{1}{2} \mu^2 \|\xi_1\|^2.$$

Without loss of generality, we assume $\|\nabla f(x)\| \neq 0$ and denote $\xi'_1 = \frac{2\langle \nabla f(x), \xi_1 \rangle}{\|\nabla f(x)\|^2} \nabla f(x) - \xi_1$. It is easy to verify that ξ'_1 also follows $\mathcal{N}(0, I_d)$, $\|\xi'_1\| = \|\xi_1\|$ and $f(x + \mu\xi_1) = f(x + \mu\xi'_1)$. Therefore, we have

$$\int_{\mathbb{R}^d} \left(\int_{f(x+\mu\xi_1) > f(x+\mu\xi_2)} p(\xi_2) d\xi_2 \right) \xi_1 p(\xi_1) d\xi_1 \quad (78)$$

$$= \int_{\mathbb{R}^d} \left(\int_{f(x+\mu\xi_1) > f(x+\mu\xi_2)} p(\xi_2) d\xi_2 \right) \xi'_1 p(\xi'_1) d\xi'_1 \quad (79)$$

$$= \frac{1}{2} \int_{\mathbb{R}^d} \left(\int_{f(x+\mu\xi_1) > f(x+\mu\xi_2)} p(\xi_2) d\xi_2 \right) (\xi_1 + \xi'_1) p(\xi_1) d\xi_1. \quad (80)$$

$$= \left(\int_{\mathbb{R}^d} \left(\int_{f(x+\mu\xi_1) > f(x+\mu\xi_2)} p(\xi_2) d\xi_2 \right) \frac{\langle \nabla f(x), \xi_1 \rangle}{\|\nabla f(x)\|} p(\xi_1) d\xi_1 \right) \frac{\nabla f(x)}{\|\nabla f(x)\|}. \quad (81)$$

Furthermore,

$$\left| \int_{\mathbb{R}^d} \left(\int_{f(x+\mu\xi_1) > f(x+\mu\xi_2)} p(\xi_2) d\xi_2 \right) \frac{\langle \nabla f(x), \xi_1 \rangle}{\| \nabla f(x) \|} p(\xi_1) d\xi_1 \right| \leq \int_{\mathbb{R}^d} \frac{|\langle \nabla f(x), \xi_1 \rangle|}{\| \nabla f(x) \|} p(\xi_1) d\xi_1 = \sqrt{\frac{2}{\pi}}. \quad (82)$$

Finally, we have

$$\left\| \mathbb{E}_{\xi_1, \xi_2} [S_f(x, \xi_1, \xi_2, \mu)(\xi_1 - \xi_2)] \right\|^2 \quad (83)$$

$$= \left\| 4 \left(\int_{\mathbb{R}^d} \left(\int_{f(x+\mu\xi_1) > f(x+\mu\xi_2)} p(\xi_2) d\xi_2 \right) \frac{\langle \nabla f(x), \xi_1 \rangle}{\| \nabla f(x) \|} p(\xi_1) d\xi_1 \right) \frac{\nabla f(x)}{\| \nabla f(x) \|} \right\|^2 \quad (84)$$

$$\leq \frac{32}{\pi}. \quad (85)$$

□

Proof of Lemma 4. We first compute that

$$E [\|\tilde{g}(x)\|_2^2] = \frac{1}{|\mathcal{E}|^2} E \left[\left\| \sum_{(i,j) \in \mathcal{E}} (\xi_j - \xi_i) \right\|_2^2 \right]. \quad (86)$$

For ease of writing, we denote $B_{(i,j)} = \xi_j - \xi_i = S_f(x, \xi_i, \xi_j, \mu)(\xi_i - \xi_j)$ and $\bar{\mathcal{E}}$ as the undirected version of \mathcal{E} .

$$E \left[\left\| \sum_{(i,j) \in \mathcal{E}} B_{(i,j)} \right\|_2^2 \right] \quad (87)$$

$$= E \left[\sum_{(i,j) \in \mathcal{E}} \|B_{(i,j)}\|_2^2 + \sum_{\substack{(i,j) \in \bar{\mathcal{E}} \\ (i',j) \in \bar{\mathcal{E}} \\ i \neq i'}} \langle B_{(i,j)}, B_{(i',j)} \rangle + \sum_{\substack{(i,j) \in \bar{\mathcal{E}} \\ (i',j') \in \bar{\mathcal{E}} \\ i \neq i', j \neq j'}} \langle B_{(i,j)}, B_{(i',j')} \rangle \right]. \quad (88)$$

With the two metrics $M_1(f, \mu)$, $M_2(f, \mu)$, we can bound the four terms in (88) as follows:

$$E [\|B_{(i,j)}\|_2^2] = E [\|\xi_j - \xi_i\|_2^2] = 2d, \quad (89)$$

$$E [\langle B_{(i,j)}, B_{(i',j)} \rangle] = E [\langle B_{(i,j)}, B_{(i',j')} \rangle] \leq M_2(f, \mu), \quad (90)$$

$$E [\langle B_{(i,j)}, B_{(i',j')} \rangle] = \|E [B_{(i,j)}]\|_2^2 \leq M_1(f, \mu). \quad (91)$$

Taking (89), (90) and (91) into (88), we obtain

$$E \left[\left\| \sum_{(i,j) \in \mathcal{E}} B_{(i,j)} \right\|_2^2 \right] \quad (92)$$

$$\leq \sum_{(i,j) \in \mathcal{E}} 2d + \sum_{\substack{(i,j) \in \bar{\mathcal{E}} \\ (i',j) \in \bar{\mathcal{E}} \\ i \neq i'}} M_2(f, \mu) + \sum_{\substack{(i,j) \in \bar{\mathcal{E}} \\ (i',j') \in \bar{\mathcal{E}} \\ i \neq i', j \neq j'}} M_1(f, \mu) \quad (93)$$

$$= 2|\mathcal{E}|d + N(\mathcal{E})M_2(f, \mu) + (|\mathcal{E}|^2 - N(\mathcal{E}) - |\mathcal{E}|)M_1(f, \mu). \quad (94)$$

Combing (94) with (86), we obtain

$$E [\|\tilde{g}(x)\|_2^2] \leq \frac{2d}{|\mathcal{E}|} + \frac{N(\mathcal{E})}{|\mathcal{E}|^2} M_2(f, \mu) + \frac{|\mathcal{E}|^2 - N(\mathcal{E}) - |\mathcal{E}|}{|\mathcal{E}|^2} M_1(f, \mu) \quad (95)$$

$$\leq \frac{2d}{|\mathcal{E}|} + \frac{N(\mathcal{E})}{|\mathcal{E}|^2} M_2(f, \mu) + M_1(f, \mu). \quad (96)$$

□

Proof of Theorem 1. Consider the t -th iteration, from L -smoothness we can know that

$$f(x_t) - f(x_{t-1}) \leq -\eta \langle \nabla f(x_{t-1}), g_t \rangle + \frac{\eta^2 L}{2} \|g_t\|_2^2. \quad (97)$$

Using Lemma 1 and Lemma 4, we have

$$\mathbb{E}[f(x_t) - f(x_{t-1})] \leq -\eta \langle \nabla f(x_{t-1}), E[g_t] \rangle + \frac{\eta^2 L}{2} E [\|g_t\|_2^2] \quad (98)$$

$$\leq -\eta \|\nabla f(x_{t-1})\| + C_d \eta \mu L + \frac{\eta^2 L}{2} \left(\frac{2d}{|\mathcal{E}|} + \frac{N(\mathcal{E})}{|\mathcal{E}|^2} M_2(f, \mu) + M_1(f, \mu) \right), \quad (99)$$

where the expectation is taken over the random direction $\xi_{(t,1)}, \dots, \xi_{(t,m)}$.

Rearrange the inequality, we have

$$\|\nabla f(x_{t-1})\| \leq \frac{\mathbb{E}[f(x_{t-1}) - f(x_t)]}{\eta} + C_d \mu L + \frac{\eta L}{2} \left(\frac{2d}{|\mathcal{E}|} + \frac{N(\mathcal{E})}{|\mathcal{E}|^2} M_2(f, \mu) + M_1(f, \mu) \right). \quad (100)$$

Sum up over T iterations and divide both sides by T , we finally obtain

$$\mathbb{E} \left[\frac{1}{T} \sum_{t=1}^T \|\nabla f(x_{t-1})\| \right] \leq \frac{\mathbb{E}[f(x_0) - f(x_T)]}{\eta T} + C_d \mu L + \frac{\eta L}{2} \left(\frac{2d}{|\mathcal{E}|} + \frac{N(\mathcal{E})}{|\mathcal{E}|^2} M_2(f, \mu) + M_1(f, \mu) \right) \quad (101)$$

$$\leq \frac{f(x_0) - f^*}{\eta T} + C_d \mu L + \frac{\eta L}{2} \left(\frac{2d}{|\mathcal{E}|} + \frac{N(\mathcal{E})}{|\mathcal{E}|^2} M_2(f, \mu) + M_1(f, \mu) \right). \quad (102)$$

The proof is completed by

$$\mathbb{E} \left[\min_{t \in \{1, \dots, T\}} \|\nabla f(x_{t-1})\| \right] \leq \mathbb{E} \left[\frac{1}{T} \sum_{t=1}^T \|\nabla f(x_{t-1})\| \right].$$

□

Proof of Lemma 5. Without loss of generality, we assume $\|\nabla f(x)\| \neq 0$. We first prove that

$$\int_{\mathcal{R}_1} \langle \nabla f(x), \xi_1 - \xi_2 \rangle p(\xi_1) p(\xi_2) d\xi_1 d\xi_2 = \frac{1}{\sqrt{\pi}} \|\nabla f(x)\|.$$

Now we denote

$$x = \frac{\langle \nabla f(x), \xi_1 - \xi_2 \rangle}{\sqrt{2} \|\nabla f(x)\|}.$$

Notice that x follows the distribution $\mathcal{N}(0, 1)$. Therefore, we have

$$\int_{\mathcal{R}_1} \langle \nabla f(x), \xi_1 - \xi_2 \rangle p(\xi_1) p(\xi_2) d\xi_1 d\xi_2 \quad (103)$$

$$= \sqrt{2} \|\nabla f(x)\| \int_{x>0} x p(x) dx = \frac{1}{\sqrt{\pi}} \|\nabla f(x)\|, \quad (104)$$

where we use a well-known fact that $\int_{x>0} xp(x)dx = \frac{1}{\sqrt{2\pi}}$.

Then we will prove

$$\int_{\mathcal{R}_{12}} \langle \nabla f(x), \xi_1 - \xi_2 \rangle p(\xi_1)p(\xi_2) d\xi_1 d\xi_2 = h(\|\nabla f(x)\|, \mu L, d).$$

Notice that

$$\mathcal{R}_{12} = \{(\xi_1, \xi_2) \mid (\xi_1, \xi_2) \in \mathcal{R}_1, \langle \nabla f(x), \xi_1 - \xi_2 \rangle - \frac{\mu L}{2} (\|\xi_1\|_2^2 + \|\xi_2\|_2^2) \geq 0\}.$$

We can see that \mathcal{R}_{12} is a ball in \mathbb{R}^{2d} :

$$\mathcal{R}_{12} = \left\{ (\xi_1, \xi_2) \mid \left\| \xi_1 - \frac{1}{\mu L} \nabla f(x) \right\|_2^2 + \left\| \xi_2 + \frac{1}{\mu L} \nabla f(x) \right\|_2^2 < \frac{2\|\nabla f(x)\|_2^2}{\mu^2 L^2} \right\}. \quad (105)$$

Now we denote $\zeta = [-\xi_1^\top, \xi_2^\top]^\top \in \mathbb{R}^{2d}$, $\phi = [\nabla f(x)^\top, \nabla f(x)^\top]^\top \in \mathbb{R}^{2d}$. Notice that ζ still follows a isotropic multivariate Gaussian distribution, we can simiplify the integral in LHS of (34) as:

$$\int_{\mathcal{S}_\zeta(\phi)} \langle \phi, \zeta \rangle p(\zeta) d\zeta \quad (106)$$

$$\text{where } \mathcal{S}_\zeta(\phi) = \left\{ \zeta \mid \left\| \zeta - \frac{1}{\mu L} \phi \right\|_2^2 < \frac{\|\phi\|_2^2}{\mu^2 L^2} \right\}.$$

We argue that for any rotation matrix $R \in \mathbb{R}^{2d \times 2d}$, i.e., $\det(R) = 1$ and $R^\top = R^{-1}$. We have

$$\int_{\mathcal{S}_\zeta(\phi)} \langle \phi, \zeta \rangle p(\zeta) d\zeta = \int_{\mathcal{S}_\zeta(R\phi)} \langle R\phi, \zeta \rangle p(\zeta) d\zeta. \quad (107)$$

To see that, we can rotate ζ by R . Denote $\zeta' = R^\top \zeta$, we first have

$$\mathcal{S}_\zeta(R\phi) = \left\{ \zeta \mid \left\| \zeta - \frac{1}{\mu L} R\phi \right\|_2^2 < \frac{\|\phi\|_2^2}{\mu^2 L^2} \right\} = \left\{ R\zeta' \mid \left\| \zeta' - \frac{1}{\mu L} \phi \right\|_2^2 < \frac{\|\phi\|_2^2}{\mu^2 L^2} \right\} = \{R\zeta' \mid \zeta' \in \mathcal{S}_{\zeta'}(\phi)\} \quad (108)$$

$$\int_{\mathcal{S}_\zeta(R\phi)} \langle R\phi, \zeta \rangle p(\zeta) d\zeta = \int_{\{R\zeta' \mid \zeta' \in \mathcal{S}_{\zeta'}(\phi)\}} \langle R\phi, R\zeta' \rangle p(R\zeta') dR\zeta' = \int_{\mathcal{S}_{\zeta'}(\phi)} \langle \phi, \zeta' \rangle p(\zeta') d\zeta', \quad (109)$$

where we use the property of $p(\cdot)$: $p(R\zeta') = p(\zeta')$.

Now we denote $\phi' = [\|\phi\|, 0, \dots, 0]^\top \in \mathbb{R}^{2d}$, it is easy to see that ϕ' is a rotated version of ϕ , i.e., there exists a rotation matrix R' such that $\phi' = R'\phi$. Denote $\zeta = [\zeta_1, \dots, \zeta_{2d}]^\top$, and $\zeta_{/1} = [\zeta_2, \dots, \zeta_{2d}]^\top$. We have

$$\int_{\mathcal{S}_\zeta(\phi)} \langle \phi, \zeta \rangle p(\zeta) d\zeta \quad (110)$$

$$= \int_{\mathcal{S}_\zeta(\phi')} \langle \phi', \zeta \rangle p(\zeta) d\zeta \quad (111)$$

$$= \|\phi\| \int_{(\zeta_1 - \frac{\|\phi\|}{\mu L})^2 + \zeta_2^2 + \dots + \zeta_{2d}^2 \leq \frac{\|\phi\|_2^2}{\mu^2 L^2}} \zeta_1 p(\zeta) d\zeta \quad (112)$$

$$= \|\phi\| \int_0^{\frac{2\|\phi\|}{\mu L}} \zeta_1 \left(\int_{\zeta_2^2 + \dots + \zeta_{2d}^2 \leq \frac{\|\phi\|_2^2}{\mu^2 L^2} - (\zeta_1 - \frac{\|\phi\|}{\mu L})^2} p(\zeta_{/1}) d\zeta_{/1} \right) p(\zeta_1) d\zeta_1. \quad (113)$$

Notice that $\zeta_2, \dots, \zeta_{2d}$ are i.i.d and following standard Gaussian distribution, and hence $\zeta_2^2 + \dots + \zeta_{2d}^2$ follows the Chi-square distribution with $2d - 1$ degrees of freedom. Therefore,

$$\int_{\mathcal{S}_\zeta(\phi)} \langle \phi, \zeta \rangle p(\zeta) d\zeta \quad (114)$$

$$= \|\phi\| \int_0^{\frac{2\|\phi\|}{\mu L}} \zeta_1 F_{2d-1} \left(\frac{\|\phi\|^2}{\mu^2 L^2} - \left(\zeta_1 - \frac{\|\phi\|}{\mu L} \right)^2 \right) p(\zeta_1) d\zeta_1 \quad (115)$$

$$= \|\phi\| \int_0^{\frac{2\|\phi\|}{\mu L}} \zeta_1 F_{2d-1} \left(\left(\frac{2\|\phi\|}{\mu L} - \zeta_1 \right) \zeta_1 \right) p(\zeta_1) d\zeta_1 \quad (116)$$

$$= \sqrt{2} \|\nabla f(x)\| \int_0^{\frac{2\sqrt{2}\|\nabla f(x)\|}{\mu L}} \zeta_1 F_{2d-1} \left(\left(\frac{2\sqrt{2}\|\nabla f(x)\|}{\mu L} - \zeta_1 \right) \zeta_1 \right) p(\zeta_1) d\zeta_1 \quad (117)$$

$$= h(\|\nabla f(x)\|, \mu L, d). \quad (118)$$

□

Proof of Lemma 6. We define the function $q(u, d) : \mathbb{R}_+ \times \mathbb{Z}_+ \rightarrow \mathbb{R}_+$ as follows:

$$q(u, d) = \int_0^{2\sqrt{2}u} x F_{2d-1} \left((2\sqrt{2}u - x) x \right) p(x) dx. \quad (119)$$

Notice that $h(v, r, d) = \sqrt{2}vq(v/r, d)$.

We first need to prove an important properties of the $q(u, d)$:

$$\lim_{u \rightarrow \infty} q(u, d) = \frac{1}{\sqrt{2\pi}}.$$

Consider an arbitrary $\epsilon > 0$. Since $\int_0^{+\infty} xp(x) dx = \frac{1}{\sqrt{2\pi}}$, there exists $N_2 > N_1 > 0$ and such that

$$0 < \int_0^{N_1} xp(x) dx \leq \frac{\epsilon}{3}, \quad (120)$$

$$0 < \int_{N_2}^{\infty} xp(x) dx \leq \frac{\epsilon}{3}. \quad (121)$$

On the other hands, for every $u > \frac{N_2}{\sqrt{2}}$, since $(2\sqrt{2}u - x) x$ is monotonely increasing on $[N_1, N_2]$, we have

$$\int_{N_1}^{N_2} x F_{2d-1} \left((2\sqrt{2}u - x) x \right) p(x) dx > F_{2d-1} \left((2\sqrt{2}u - N_1) N_1 \right) \int_{N_1}^{N_2} xp(x) dx. \quad (122)$$

Notice that

$$\lim_{u \rightarrow \infty} F_{2d-1} \left((2\sqrt{2}u - N_1) N_1 \right) = 1,$$

there must exist a number N_3 such that if $u > N_3$, then

$$F_{2d-1} \left((2\sqrt{2}u - N_1) N_1 \right) > 1 - \sqrt{2\pi}\epsilon. \quad (123)$$

Putting together (122) and (123), because $0 \leq F_{2d-1} \left((2\sqrt{2}u - x) x \right) \leq 1$, if $u > \max\{\frac{N_2}{\sqrt{2}}, N_3\}$, we can obtain

$$0 < \int_0^{+\infty} xp(x)dx - \int_0^{2\sqrt{2}u} xF_{2d-1} \left((2\sqrt{2}u - x) x \right) p(x)dx \quad (124)$$

$$\leq \frac{2\epsilon}{3} + \int_{N_1}^{N_2} xp(x)dx - \int_{N_1}^{N_2} xF_{2d-1} \left((2\sqrt{2}u - x) x \right) p(x)dx \quad (125)$$

$$\leq \frac{2\epsilon}{3} + \int_{N_1}^{N_2} xp(x)dx - F_{2d-1} \left((2\sqrt{2}u - N_1) N_1 \right) \int_{N_1}^{N_2} xp(x)dx \quad (126)$$

$$\leq \frac{2\epsilon}{3} + \int_{N_1}^{N_2} xp(x)dx - \left(1 - \sqrt{2\pi}\epsilon \right) \int_{N_1}^{N_2} xp(x)dx \quad (127)$$

$$= \frac{2\epsilon}{3} + \frac{\epsilon}{3} \int_{N_1}^{N_2} xp(x)dx < \frac{2\epsilon}{3} + \sqrt{2\pi}\epsilon \frac{1}{\sqrt{2\pi}} = \epsilon. \quad (128)$$

Taking $\epsilon \rightarrow 0$, hence we know that

$$\lim_{u \rightarrow \infty} q(u, d) = \int_0^{+\infty} xp(x)dx = \frac{1}{\sqrt{2\pi}}.$$

Since $\lim_{u \rightarrow \infty} q(u, d) = \frac{1}{\sqrt{2\pi}}$, there exists a constant C_d such that whenever $\left(\frac{1}{2\sqrt{\pi}} + \frac{1}{4} \right) u > \frac{1}{4}C_d$, we have

$$q(u, d) \geq \frac{1}{\sqrt{2\pi}} - \left(\frac{1}{2\sqrt{2\pi}} - \frac{1}{4\sqrt{2}} \right) = \frac{1}{2\sqrt{2\pi}} + \frac{1}{4\sqrt{2}}. \quad (129)$$

Therefore, whenever $\left(\frac{1}{2\sqrt{\pi}} + \frac{1}{4} \right) v > \frac{1}{4}C_d r$, we have

$$h(v, r, d) = \sqrt{2}vq(v/r, d) \geq \left(\frac{1}{2\sqrt{\pi}} + \frac{1}{4} \right) v \geq \left(\frac{1}{2\sqrt{\pi}} + \frac{1}{4} \right) v - \frac{1}{4}C_d r. \quad (130)$$

On the other hand, when $\left(\frac{1}{2\sqrt{\pi}} + \frac{1}{4} \right) v \leq \frac{1}{4}C_d r$, we have

$$h(v, r, d) = \sqrt{2}vq(v/r, d) \geq 0 \geq \left(\frac{1}{2\sqrt{\pi}} + \frac{1}{4} \right) v - \frac{1}{4}C_d r. \quad (131)$$

□

C Experiment details

C.1 Hyperparameter choices for the experiments in Section 4.1.

Figure 8 and 9 show the performance of tested algorithms in Figure 3 under different hyperparameter settings. For gradient-based algorithms, ZO-SGD, SCBO and ZO-RankSGD, we tune the stepsize and set $\gamma = 0.1$ for the line search. We need to remark that when implementing the SCBO [3], we remove the sparsity constraint because we found that it will lead to degraded performance for non-sparse problems like the ones we tested. For GLD-Fast, we tune for the diameter of search sparse, denoted as μ . For CMA-ES, we tune for the initial variance, also denoted as μ in the figures. To run the experiment in Figure 3, we select the optimal choices of hyperparameters based on Figure 8 and 9 for each algorithm, respectively.

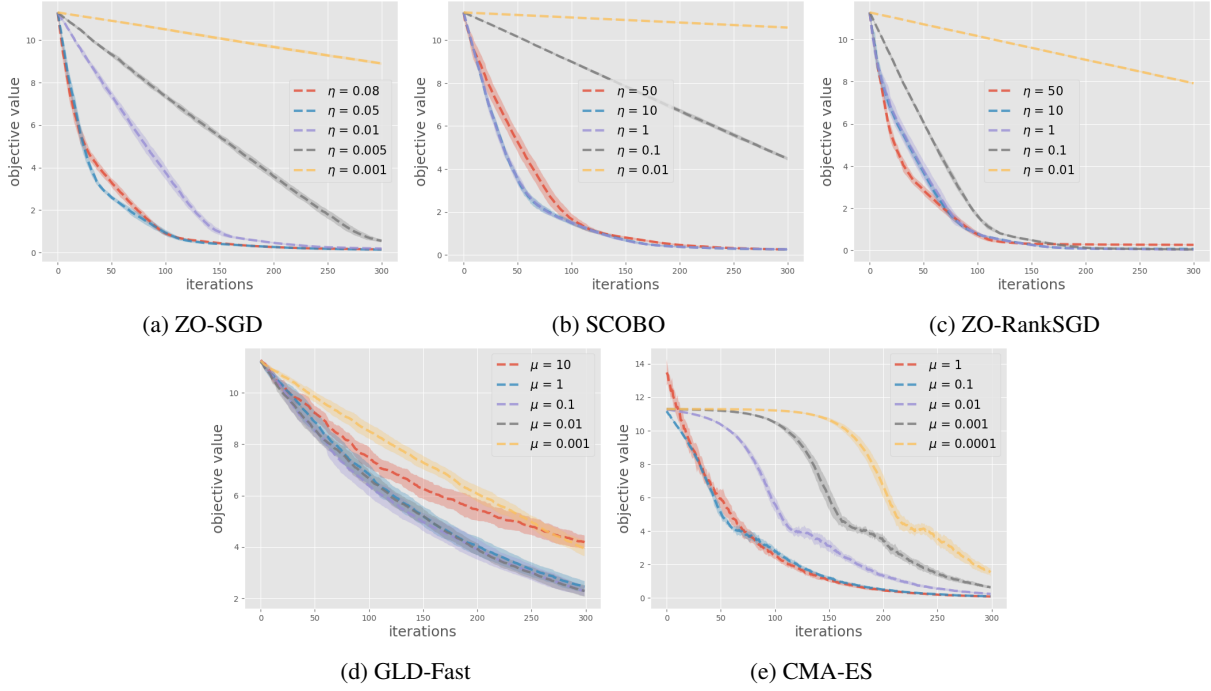


Figure 8: Hyperparameter tuning on Quadratic function.

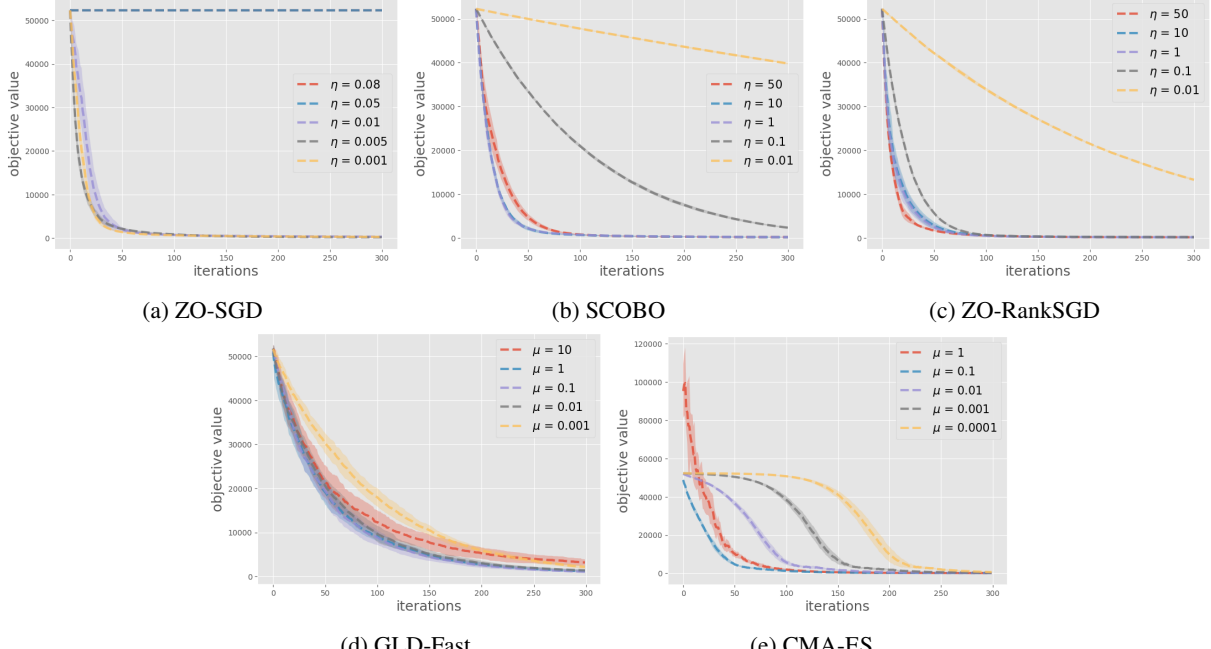


Figure 9: Hyperparameter tuning on Rosenbrock function.

C.2 Details for the experiment in Section 4.3.

Modified ZO-RankSGD algorithm for optimizing latent embeddings of Stable Diffusion. To enhance the efficiency of Algorithm 1, we make a modification to preserve the best image obtained during the optimization process. Specifically, in the original algorithm, the best point among all queried images is not saved, which can lead to inefficiencies. Therefore, we modify the algorithm to store the best point in the gradient estimation step as x^{**} and add it to

the later line search step. This modification can be viewed as a combination of ZO-RankSGD and Direct Search [26]. Another useful feature of Algorithm 3 is that if the best point is not updated in the line search step, the algorithm returns to the gradient estimation step to form a more accurate gradient estimator. The modified algorithm is presented in Algorithm 3. At every iteration in Algorithm 3, we evaluate the latent embeddings by passing them to the DPM-solver with Stable Diffusion and then ask human or CLIP model to rank the generated images.

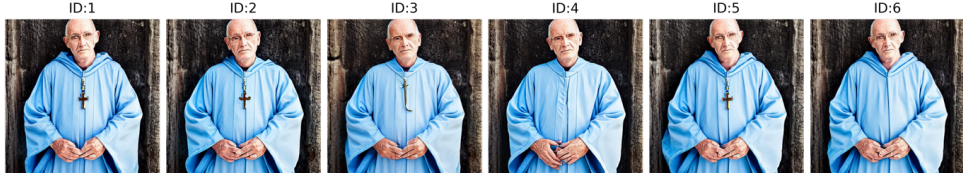
Algorithm 3 Modified ZO-RankSGD algorithm for optimizing latent embeddings of Stable Diffusion.

Require: Objective function f (Evaluated by human or CLIP model), initial point x_0 , number of queries m , stepsize η , smoothing parameter μ , shrinking rate $\gamma \in (0, 1)$, number of trials l .

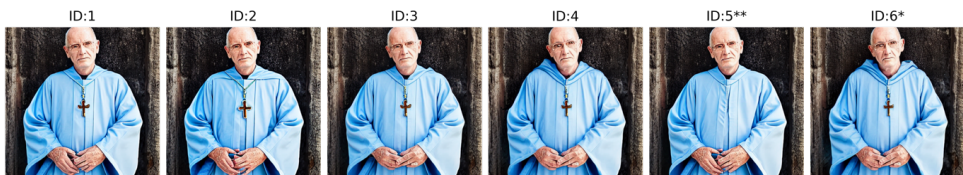
- 1: Initialize the best point $x^* = x_0$.
- 2: Initialize the gradient memory \bar{g} with all-zero vectors.
- 3: Set $\tau = 0$.
- 4: **while** not terminated by user **do**
- 5: Sample m i.i.d. direction $\{\xi_1, \dots, \xi_m\}$ from $N(0, I)$.
- 6: Query $O_f^{(m,k)}$ with input $\mathcal{X}_1 = \{x^* + \mu\xi_1, \dots, x^* + \mu\xi_m\}$ for some $k \leq m$. Denote \mathbb{I}_1 as the output.
- 7: Set x^{**} to be the point in \mathcal{X}_1 with minimal objective value.
- 8: Compute the gradient \hat{g} using the ranking information \mathbb{I}_1 as in Algorithm 1.
- 9: $\bar{g} = (\tau\bar{g} + \hat{g})/(\tau + 1)$
- 10: $\tau = \tau + 1$
- 11: Query $O_f^{(m,1)}$ with input $\mathcal{X}_2 = \{x^*, x^{**}, x^* - \eta\bar{g}, x^* - \eta\gamma\bar{g}, \dots, x^* - \eta\gamma^{m-2}\bar{g}\}$. Denote \mathbb{I}_2 as the output.
- 12: **if** $1 \in \mathbb{I}_2$, i.e., x^* has the minimal objective value **then**
- 13: Go back to line 5.
- 14: **else**
- 15: Set x^* to be the point in \mathcal{X}_2 with minimal objective value.
- 16: Initialize the gradient memory \bar{g} with all-zero vectors.
- 17: Set $\tau = 0$.
- 18: **end if**
- 19: **end while**

The User Interface for Algorithm 3. Figure 10 presents the corresponding user interface (UI) designed for collecting human feedback in Algorithm 3, where 6 images are presented to the users at each round. When the user receives the instruction "Please rank the following image from best to worst," it indicates that the algorithm is in the gradient estimation step. In this case, users are required to rank k best images, where k can be any number they choose. Then, the user receives the instruction "Please input the ID of the best image," indicating that the algorithm has moved to the line search step, and users only need to choose the best image from the presented images. This interface enables easy and intuitive communication between the user and the algorithm, facilitating the optimization process.

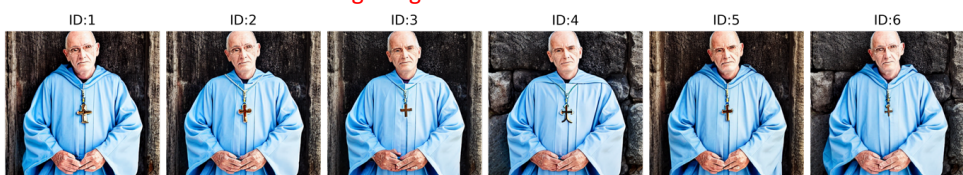
Round 1: Please rank the following image from best to worst -> 4 2 1 5 3 6



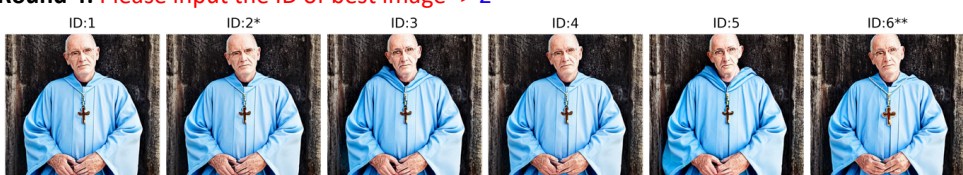
Round 2: Please input the ID of best image -> 1



Round 3: Please rank the following image from best to worst -> 2 6 1 3 5 4

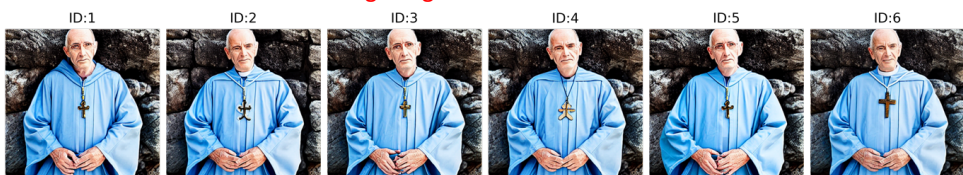


Round 4: Please input the ID of best image -> 2



⋮
⋮

Round 13: Please rank the following image from best to worst -> 6 3 1 5



Round 14: Please input the ID of best image -> 6



Round 15: Exit

Figure 10: The User Interface of Algorithm 3.

More examples like the ones in Figure 7 are presented in Figure 11.

Other details. For all the examples in Figure 7 and Figure 11, we set the number of rounds for human feedback between 10 and 20, which was determined based on our experience with the optimization process. For the images obtained from the CLIP similarity score, we fixed the number of querying rounds to 50. Both the optimization from human feedback and CLIP similarity score used the same parameters for Algorithm 3: $\eta = 1$, $\mu = 0.1$, and $\gamma = 0.5$.

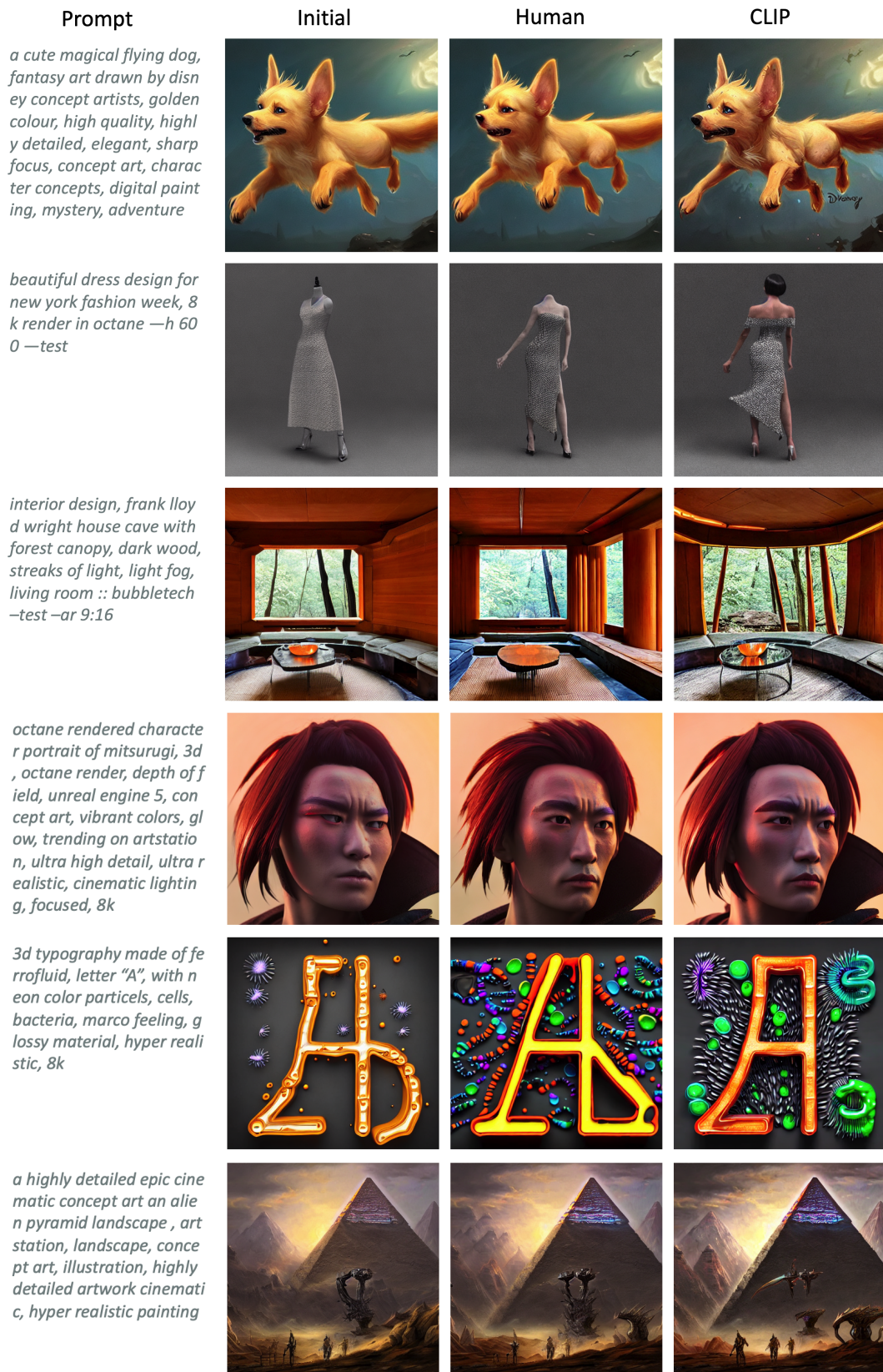


Figure 11: More examples.